MicroRNA-181b regulates NF-κB–mediated vascular inflammation

Xinghui Sun,[1] Basak Icli,[1] Akm Khyrul Wara,[1] Nathan Belkin,[1] Shaolin He,[1] Lester Kobzik,[2] Gary M. Hunninghake,[3] Miguel Pinilla Vera,[3] MICU Registry,[3] Timothy S. Blackwell,[4] Rebecca M. Baron,[3] and Mark W. Feinberg[1]

[1]Department of Medicine, Cardiovascular Division, [2]Department of Pathology, and [3]Department of Medicine, Pulmonary and Critical Care Division, Brigham and Women's Hospital, Harvard Medical School, Boston, Massachusetts, USA. [4]Department of Medicine, Division of Allergy, Pulmonary and Critical Care Division, Vanderbilt University School of Medicine, Nashville, Tennessee, USA.

EC activation and dysfunction have been linked to a variety of vascular inflammatory disease states. The function of microRNAs (miRNAs) in vascular EC activation and inflammation remains poorly understood. Herein, we report that microRNA-181b (miR-181b) serves as a potent regulator of downstream NF-κB signaling in the vascular endothelium by targeting importin-α3, a protein that is required for nuclear translocation of NF-κB. Overexpression of miR-181b inhibited importin-α3 expression and an enriched set of NF-κB–responsive genes such as adhesion molecules VCAM-1 and E-selectin in ECs in vitro and in vivo. In addition, treatment of mice with proinflammatory stimuli reduced miR-181b expression. Rescue of miR-181b levels by systemic administration of miR-181b "mimics" reduced downstream NF-κB signaling and leukocyte influx in the vascular endothelium and decreased lung injury and mortality in endotoxemic mice. In contrast, miR-181b inhibition exacerbated endotoxin-induced NF-κB activity, leukocyte influx, and lung injury. Finally, we observed that critically ill patients with sepsis had reduced levels of miR-181b compared with control intensive care unit (ICU) subjects. Collectively, these findings demonstrate that miR-181b regulates NF-κB–mediated EC activation and vascular inflammation in response to proinflammatory stimuli and that rescue of miR-181b expression could provide a new target for antiinflammatory therapy and critical illness.

Introduction

The vascular endothelium represents a critical interface between blood and all tissues. Endothelial dysfunction contributes to the development of both acute inflammatory disease states, such as endotoxemia and sepsis, and chronic inflammatory disease states, such as atherosclerosis, diabetes, rheumatoid arthritis, and inflammatory bowel disease (1–8). In response to inflammatory stimuli, the vascular endothelium expresses a number of adhesion molecules that play key roles in the recruitment of leukocytes to sites of inflammation (9, 10). In particular, vascular cell adhesion molecule 1 (VCAM-1), E-selectin, and intercellular adhesion molecule 1 (ICAM-1) mediate early leukocyte attachment and rolling events. An inflammatory response within tissues is subsequently generated after events, such as firm adhesion and transmigration, occur (9). Clinical studies have found that the soluble forms of these adhesion molecules are increased in patients experiencing vascular inflammatory disease (11, 12).

Induction of VCAM-1, E-selectin, and ICAM-1 in ECs is primarily mediated by the activation of the NF-κB pathway (13–17). Activation of NF-κB transcription factors has been implicated in many physiological and pathological processes (3, 18, 19). The transcriptional activity of NF-κB can be induced by a variety of stimuli, including proinflammatory cytokines TNF-α and IL-1β, exposure to bacterial products such as LPS, engagement of the T cell receptor, or stimulation of the CD40 and lymphotoxin-β receptors (19). In the canonical NF-κB signaling pathway, stimulus-mediated activation of IκB kinase (IKK) complex leads to IKK rapidly phosphorylating IκBα at 2 N-terminal serines, which in turn results in its ubiquitin-induced degradation by the 26S proteasome (20). This event then leads to the release of NF-κB heterodimers, which then translocate to the nucleus via importin proteins and drive a wide range of gene expression by binding to various κB elements. In the vascular endothelium, activation of NF-κB leads to the expression of proinflammatory genes, including those encoding cytokines, adhesion molecules, and chemoattractant proteins that together play critical roles in all aspects of the inflammatory and immune responses (21–26). Thus, targeting NF-κB–mediated EC activation holds promise for the development of novel antiinflammatory therapies.

miRNAs are emerging as new regulators of inflammatory and immune responses (27, 28). miRNAs are a class of single-stranded, small, noncoding RNAs that typically bind to the 3′ UTR of target mRNA sequences, an effect leading to the reduction of protein expression predominantly by destabilizing target mRNAs and/or by translation inhibition (29–32). While over 1,000 human mature miRNA sequences are listed in the miRNA registry (33), only a handful have been characterized as functional regulators of leukocyte or EC inflammatory responses (28, 34, 35). In this study, we present data identifying microRNA-181b (miR-181b) as an essential regulator of downstream NF-κB signaling, EC activation, and vascular inflammation in vivo by direct targeting of importin-α3, a protein critical for NF-κB nuclear translocation. These results may provide insights into the pathophysiology of a number of acute and chronic inflammatory disease states associated with dysregulated NF-κB signaling.

Results

miR-181b expression in ECs is regulated by TNF-α. In an attempt to identify how proinflammatory stimuli regulate endothelial func-

Conflict of interest: Mark W. Feinberg, Xinghui Sun, and Brigham and Women's Hospital have a patent pending related to the work that is described in the present study.

Citation for this article: *J Clin Invest.* 2012;122(6):1973–1990. doi:10.1172/JCI61495.

tion, microarray miRNA profiling studies were undertaken using RNA from HUVECs exposed to vehicle alone or TNF-α for 4 hours, and reduced expression of miR-181b was noted (Supplemental Figure 1A; supplemental material available online with this article; doi:10.1172/JCI61495DS1). Using real-time PCR analysis, we verified that miR-181b was rapidly reduced in response to TNF-α at 1 and 4 hours by 31% and 24%, respectively (Figure 1A), whereas at 24 hours, miR-181b expression increased before returning to baseline (Supplemental Figure 1B). miR-181b belongs to the miR-181 family, which comprises 4 mature miRNAs: miR-181a, miR-181b, miR-181c, and miR-181d. These mature sequences are encoded by 6 primary miRNA sequences located on 3 different chromosomes. The expression of miR-181b was determined to be about 12-fold higher than that of miR-181a and 274-fold higher than that of miR-181c by real-time PCR (Figure 1B). Since the level of primary miR-181d was very low (data not shown), we did not examine the level of this mature miR-181d. Collectively, these data suggest that miR-181b is the dominantly expressed miR-181 family member in HUVECs and that its expression is rapidly reduced in response to stimulation by the inflammatory cytokine TNF-α.

miR-181b inhibits TNF-α–induced expression of adhesion molecules and inhibits leukocyte adhesion to activated EC monolayers. To assess the potential role of miR-181b in endothelial activation, we examined the effect of miR-181b on TNF-α–induced gene expression in HUVECs by using gain- and loss-of-function experiments. Overexpression of miR-181b inhibited TNF-α–induced VCAM-1, E-selectin, and ICAM-1 protein expression by 78%, 54%, and 44%, respectively, while miR-181b inhibitors (complementary antagonist) increased their expression by 122%, 81%, and 48%, respectively (Figure 1C and Supplemental Figure 1G). In agreement with these results, the mRNA levels of *VCAM-1*, *E-selectin*, and *ICAM-1* were lower in cells overexpressing miR-181b than in cells overexpressing the miRNA negative control; moreover, these mRNA levels were higher in the presence of the miR-181b inhibitor (Figure 1D). After 1 hour of TNF-α treatment, cells overexpressing miR-181b exhibited reduced mRNA levels of *VCAM-1*, *E-selectin*, and *ICAM-1* (by 69%, 65%, and 57%, respectively); after 4 hours of TNF-α treatment, the levels were 74%, 41%, and 17%, respectively. In contrast, in cells transfected with miR-181b inhibitors, TNF-α–induced *VCAM-1* mRNA was increased by 62% after 1 hour of TNF-α treatment, and after 4 hours of TNF-α treatment, *VCAM-1*, *E-selectin*, and *ICAM-1* mRNA levels were increased by 35%, 52%, and 34%, respectively (Figure 1D). The effects of miR-181b on levels of soluble VCAM-1, E-selectin, and ICAM-1 in the culture medium, as measured by ELISA, were also consistent with its effects on the mRNA and protein expression of these adhesion molecules (Figure 1E). Likewise, miR-181b also reduced VCAM-1 expression at both the protein and mRNA levels in HUVECs in response to LPS treatment (Supplemental Figure 1, C–E). Similar effects on VCAM-1 expression were observed for miR-181a (data not shown). Considering our finding that VCAM-1 expression was most sensitive to miR-181b, we determined whether the VCAM-1 gene might be a direct target of the miRNA. However, overexpression of miR-181b did not alter the luciferase activity of a VCAM-1 3′ UTR construct, suggesting that the VCAM-1 3′ UTR is not directly targeted by miR-181b (Supplemental Figure 1F). Since VCAM-1, E-selectin, and ICAM-1 are typical proinflammatory molecules induced by TNF-α (14, 15, 36–38), these data suggested that miR-181b may be involved in the regulation of EC activation. In response to EC activation, adhesion molecules, such as VCAM-1, E-selectin, and ICAM-1, act to initiate, promote, and sustain leukocyte attachment to the vascular endothelium. To determine the functional consequence of miR-181b effects on adhesion molecule expression, we employed an in vitro cell adhesion assay to assess leukocyte-EC interactions. As expected, TNF-α treatment markedly increased the adhesion capabilities of THP-1 cells to HUVECs transfected with miRNA negative control. However, adhesion was markedly reduced (by 44%) with miR-181b overexpression, whereas inhibition of miR-181b increased the adherence by 50% (Figure 1F). Taken together, these findings suggest that miR-181b is able to negatively affect the expression of key adhesion molecules induced by proinflammatory stimuli and that miR-181b dynamically regulates leukocyte adhesion to stimulated EC monolayers.

miR-181b suppresses TNF-α–induced expression of adhesion molecules in vivo. We next investigated whether systemic administration of miR-181b could inhibit TNF-α–induced gene expression in vivo. To assess the effects of miR-181b mimics on TNF-α–induced expression of VCAM-1 in vivo, miR-181b or a miRNA negative control (1 nmol/mouse) was admixed with atelocollagen and tail vein injected 24 hours prior to TNF-α treatment. VCAM-1 protein expression was first examined in lung tissues. At 4 hours after TNF-α i.p. injection, VCAM-1 was found to be induced by approximately 3.4-fold in lung tissues in the presence of NS control mimics. In contrast, administration of miR-181b potently reduced the induction of VCAM-1 protein expression (Figure 2A) and *VCAM-1* mRNA expression in lung, aorta, heart, liver, and spleen (Figure 2B). The expression of *E-selectin* mRNA was also significantly reduced in lung, liver, and spleen (Supplemental Figure 2A), whereas *ICAM-1* mRNA was reduced only in spleen (Supplemental Figure 2B). To further verify the observed effects on VCAM-1 expression, sections of lung and descending aorta were examined by immunohistochemical techniques. The endothelium of lung and aorta from mice injected with miRNA negative control displayed robust VCAM-1 expression in response to TNF-α (Figure 2, C–E). In contrast, systemic administration of miR-181b mimics reduced the induction of VCAM-1 expression in the endothelium in lung and aorta (by ~86% and ~80%, respectively) (Figure 2, C–E). Notably, the expression of miR-181b in the intima of aortae excised from mice injected with miR-181b was approximately 8-fold higher than in mice injected with miRNA negative control, as measured by real-time quantitative PCR (qPCR) (Supplemental Figure 2C). There were no significant differences in miR-181b expression levels in the media and adventitia excised from mice injected with miR-181b or miRNA negative control (Supplemental Figure 2C). Molecular ultrasound imaging using targeted microbubbles as a contrast agent has become a useful approach for noninvasive monitoring of the expression of adhesion molecules in vivo (39–42). We used this technique to further determine the effect of miR-181b on TNF-α–induced VCAM-1 expression in vivo. The innominate artery was selected for imaging as shown in Figure 2F. We first verified that VCAM-1–targeted MicroMarker ultrasound contrast showed a low level of signal-targeted enhancement in the innominate artery at baseline (Figure 2G). In response to TNF-α, compared with mice injected with control miRNA (Figure 2H), mice injected with miR-181b (Figure 2I) exhibited a marked reduction in differential signal–targeted enhancement values for VCAM-1 as quantified in Figure 2J. In summary, these data demonstrate that systemically administered miR-181b mimics were efficiently enriched in ECs and inhibited expression of TNF-α–induced adhesion molecules in vivo.

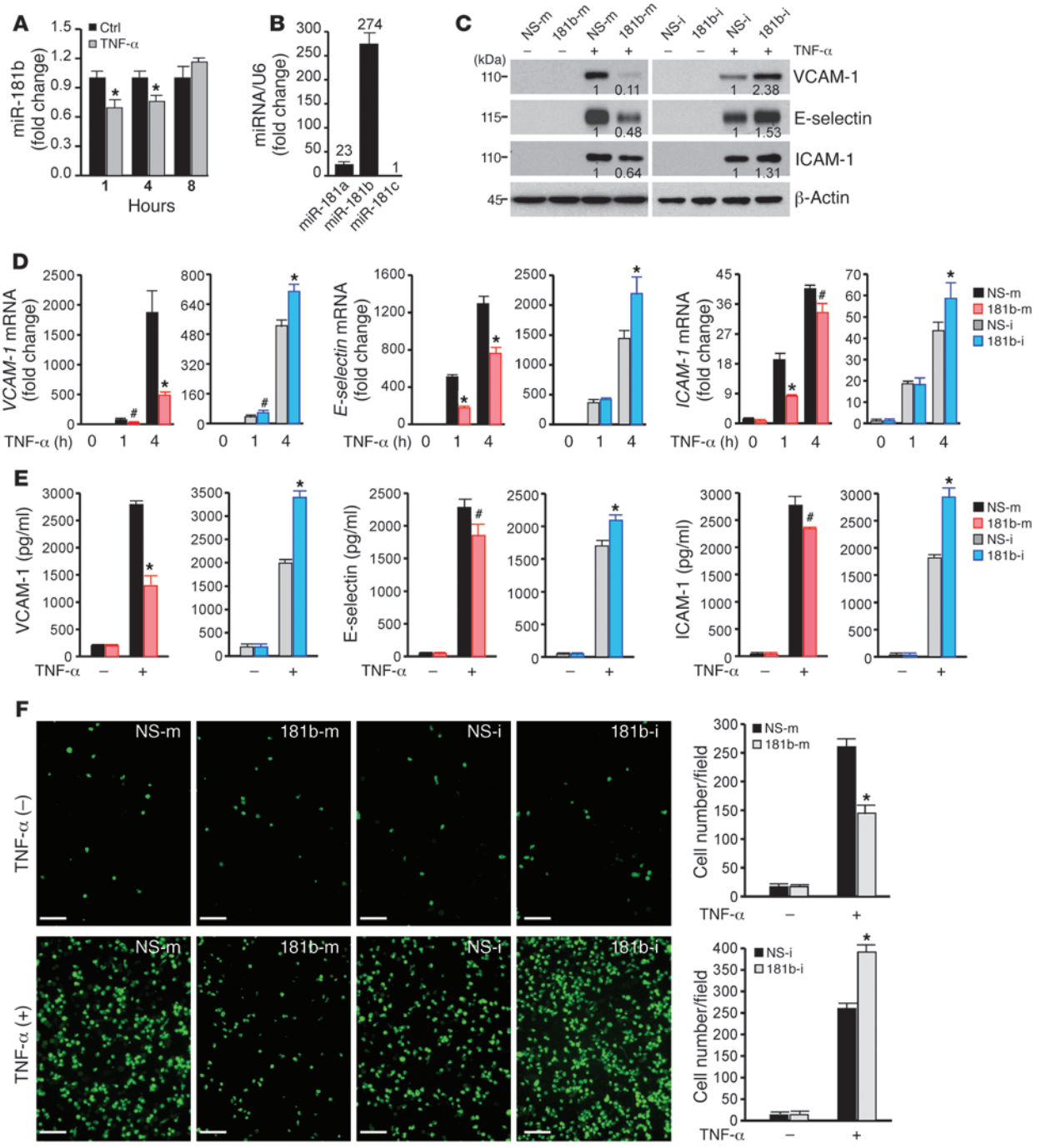

Figure 1

miR-181b suppresses TNF-α–induced proinflammatory gene expression in HUVECs. (**A**) Real-time qPCR analysis of miR-181b in response to TNF-α (10 ng/ml) in HUVECs. (**B**) Real-time qPCR analysis of miR-181a, miR-181b, and miR-181c in HUVECs. Numbers over bars indicate fold change relative to miR-181c. (**C**) Western blot analysis of VCAM-1, E-selectin, and ICAM-1 in HUVECs transfected with miRNA negative control (NS-m) or miR-181b mimics (181b-m), miRNA inhibitor negative control (NS-i), or miR-181b inhibitor (181b-i), respectively, after treatment with 10 ng/ml TNF-α for 8 hours. Densitometry was performed and fold change of protein expression is shown below the corresponding band. (**D**) Real-time qPCR analysis of *VCAM-1*, *E-selectin*, and *ICAM-1* mRNA levels in HUVECs transfected with miRNA negative control, miR-181b mimics, miRNA negative control, or miR-181b inhibitor, and treated with 10 ng/ml TNF-α for the indicated times. (**E**) ELISA analysis of elaborated VCAM-1, E-selectin, and ICAM-1 protein levels in cell culture medium 16 hours after TNF-α (10 ng/ml) treatment. HUVECs were transfected as indicated in **A**. (**F**) miR-181b regulates the adhesion of THP-1 cells to TNF-α–activated HUVECs. Photo images of THP-1 cells adhering to HUVECs transfected with miRNA negative control or miR-181b mimics, miRNA inhibitor negative control, or miR-181b inhibitor with or without 10 ng/ml TNF-α treatment for 4 hours. $^{\#}P < 0.05$; $^{*}P < 0.01$. Scale bars: 100 μm. All values represent mean ± SD.

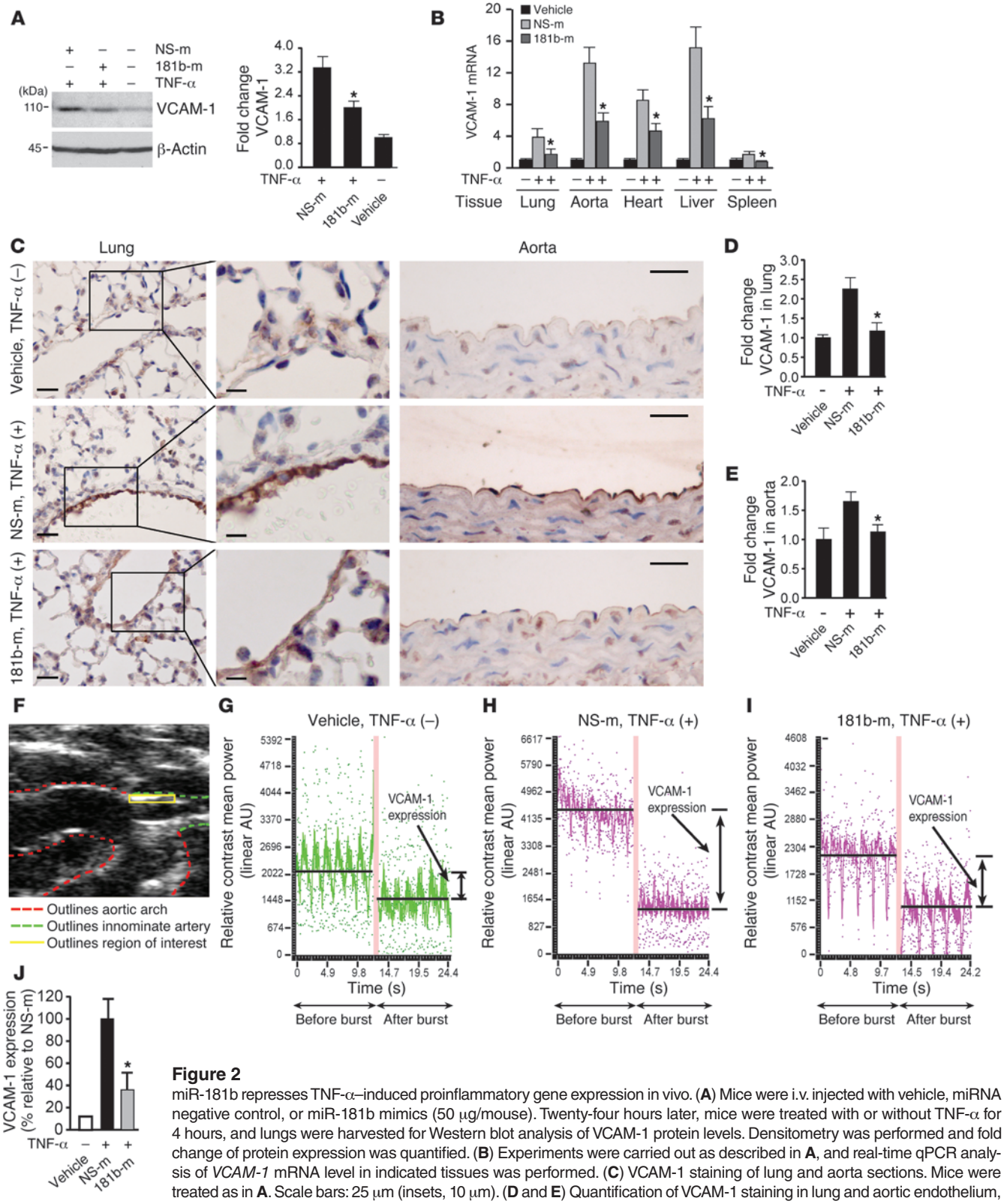

Figure 2

miR-181b represses TNF-α–induced proinflammatory gene expression in vivo. (**A**) Mice were i.v. injected with vehicle, miRNA negative control, or miR-181b mimics (50 μg/mouse). Twenty-four hours later, mice were treated with or without TNF-α for 4 hours, and lungs were harvested for Western blot analysis of VCAM-1 protein levels. Densitometry was performed and fold change of protein expression was quantified. (**B**) Experiments were carried out as described in **A**, and real-time qPCR analysis of *VCAM-1* mRNA level in indicated tissues was performed. (**C**) VCAM-1 staining of lung and aorta sections. Mice were treated as in **A**. Scale bars: 25 μm (insets, 10 μm). (**D** and **E**) Quantification of VCAM-1 staining in lung and aortic endothelium, respectively. (**A**–**E**) Vehicle group (n = 3 mice), miRNA negative control group (n = 5 mice), miR-181b mimics group (n = 5 mice). Data represent mean ± SEM. (**F**) Ultrasound image shows region of interest (innominate artery) for in vivo VCAM-1 imaging using microbubble contrast. (**G**–**I**) Mice were injected with vehicle, miRNA negative control (n = 7), or miR-181b mimics (n = 6). Representative images show the differential targeted enhancement values for VCAM-1 expression detected by ultrasound before and after microbubble burst. (**J**) Quantification of differential targeted enhancement values for VCAM-1 expression in mice injected with miRNA negative control or miR-181b mimics. Data represent mean ± SEM. *P < 0.05.

miR-181b inhibits the NF-κB signaling pathway in activated ECs. In response to proinflammatory stimuli, both the NF-κB and MAPK pathways are involved in the inflammatory responses in ECs (21, 43). To determine whether miR-181b affects NF-κB activation, we first tested to determine whether miR-181b has any effect on the NF-κB concatemer and VCAM-1 promoter-reporter. As shown in Figure 3A, treatment of HUVECs with TNF-α induced the activity of both the NF-κB concatemer and the VCAM-1 promoter-reporter, and cotransfection of miR-181b significantly attenuated this induction. In contrast, inhibition of miR-181b potentiated TNF-α–induced activity (Figure 3A). We next explored the effect of miR-181b on NF-κB nuclear accumulation by immunostaining for p65. We observed a nearly 40% reduction in p65 nuclear staining in HUVECs transfected with miR-181b as compared with cells transfected with a miRNA-negative control (Figure 3B). After its release from the IκB complex, translocation of NF-κB from the cytoplasm to the nucleus is an essential step for the activation of NF-κB target genes (44, 45), an effect that can be revealed by detection of the p50 and p65 protein levels in cytoplasmic and nuclear fractions. As shown in Figure 3, C and D, HUVECs overexpressing miR-181b exhibited reduced p65 and p50 expression by 39% and 28%, respectively, in the nuclear fraction, whereas the cytoplasmic fraction had increased p65 and p50 expression by 35% and 37%, respectively. Importantly, we did not observe any significant differences between miR-181b and the miRNA negative control on the expression of upstream components of the NF-κB pathway, including phosphorylated IκBα (in the presence or absence of proteosome inhibitor MG-132), total IκBα, or phosphorylated IKKβ (Figure 3E and Supplemental Figure 3A) in response to TNF-α, suggesting that it is unlikely that miR-181b affects cell-surface receptors or activation of the IKK complex. Since several MAPKs have been implicated in TNF-α–induced expression of adhesion molecules (46–48), we next asked whether miR-181b had any effect on the activation of 3 MAPKs (ERK, p38, and JNK) in response to TNF-α. As shown in Supplemental Figure 3B, the phosphorylation of ERK, p38, and JNK was robustly induced and peaked at 15 minutes after TNF-α treatment. However, miR-181b overexpression had no inhibitory effect on their phosphorylation at 5, 15, and 30 minutes after TNF-α treatment. These data suggest that the inhibitory role of miR-181b on TNF-α–induced gene expression is primarily due to its effects on the NF-κB signaling pathway by repression of NF-κB nuclear translocation.

miR-181b directly targets expression of importin-α3, a protein critical for NF-κB nuclear translocation. Previous studies have shown that NF-κBs are transported into the nucleus via a subset of importin-α molecules (49, 50). Because miR-181b overexpression had no effect on upstream phosphorylated IκBα or IKKβ expression, we hypothesized that miR-181b may inhibit downstream NF-κB signaling by targeting importin-α family members. There are 6 importin-α paralogs in humans (importin-α1, -α3, -α4, -α5, -α6, and -α7) that are characterized by distinct affinities to their substrates (51). Among these molecules, only importin-α3 and importin-α5 are predicted to be miR-181b targets, according to the algorithms of TargetScan (52), PITA (53), and miRanda (54). In miR-181b–overexpressing cells, importin-α3 expression, but not that of importin-α1 or importin-α5, was reduced by 40% and 25%, respectively, in the presence or absence of TNF-α (Figure 4A). Overexpression of miR-181b inhibited the activity of a luciferase reporter construct containing importin-α3 3′ UTR in a dose-dependent manner (Figure 4B). In contrast, the activity of luciferase constructs containing the 3′ UTR of importin-α1, -α4, or -α5 was not inhibited by overexpressed miR-181b (Figure 4C).

The rna22 miRNA target detection and predication algorithm allows for seed mismatches between mature miRNA and targeting mRNA sequence (55) and has been successfully used to identify direct targets that were not predicted by other algorithms (56). To identify additional miR-181b–binding sites that may exist in the 3′ UTR of importin-α3, we applied the rna22 prediction algorithm and found 8 potential miR-181b–binding sites in the region of interest (Supplemental Figure 4A). Overexpression of miR-181b decreased luciferase activity by 31% and 20%, respectively, for luciferase-reporter constructs containing binding site 1 and site 2, but not for any of the other potential binding sites (Figure 4D). Site-directed mutations of binding site 1 and site 2 rescued the miR-181b–mediated inhibitory effects on both of these constructs (Figure 4D). While site 1 has imperfect complementarity to miR-181b, it is evolutionarily conserved across species (Supplemental Figure 4B). Interestingly, the mRNA level of importin-α3 was not altered by miR-181b overexpression (Supplemental Figure 4C), an effect indicating that the reduction of importin-α3 at the protein level is likely due to translation inhibition and not mRNA decay. To further verify that miR-181b directly targets importin-α3, we performed Argonaute2 (AGO2) micro-ribonucleoprotein IP (miRNP-IP) studies to assess whether importin-α3 mRNA is enriched in the RNA-induced silencing complex following miR-181b overexpression. An approximately 4-fold enrichment of importin-α3 mRNA was observed after AGO2 miRNP-IP in the presence of miR-181b, as compared with that with the miRNA-negative control (Figure 4E). In contrast, AGO2 miRNP-IP did not enrich the mRNA for *Smad1*, a gene that was not predicted to be an miR-181b target (Figure 4E). Moreover, expression of importin-α3 lacking its 3′ UTR was able to rescue the inhibitory effect of miR-181b on NF-κB activation (Figure 4F). Systemic delivery of miR-181b also reduced importin-α3 expression by 40% in aortic endothelium (Figure 4G) and nearly 50% in lung ECs (Figure 4H). Conversely, inhibition of miR-181b increased importin-α3 expression by approximately 40% in HUVECs (Supplemental Figure 4E) and approximately 50% in the lungs in vivo (Figure 4I). To explore whether "knockdown" of importin-α3 expression could "phenocopy" the inhibitory effects of miR-181b on NF-κB, we systemically delivered importin-α3 siRNA by tail-vein injections. As shown in Supplemental Figure 5, A and B, importin-α3 siRNA reduced *importin-α3* mRNA and protein expression in freshly isolated lung ECs. Importantly, importin-α3 siRNA reduced NF-κB targets VCAM-1 and E-selectin (Supplemental Figure 5, C and D) and NF-κB activity in the lungs in vivo (Supplemental Figure 5E) as well as VCAM-1 and E-selectin expression in HUVECs in vitro (Supplemental Figure 5, F and G). Moreover, systemic delivery of importin-α3 lacking its 3′ UTR was capable of rescuing the miR-181b–mediated inhibitory effect on VCAM-1 and E-selectin expression and NF-κB activity in the lungs of mice treated with LPS (Supplemental Figure 5, H and I). In HUVECs, overexpression of importin-α3 lacking its 3′ UTR also rescued the miR-181b–mediated reduced expression for VCAM-1 and E-selectin compared with control (Supplemental Figure 5, J and K). Collectively, these data indicate that miR-181b inhibits the NF-κB signaling pathway by directly targeting importin-α3 expression.

miR-181b inhibited an enriched set of NF-κB–regulated genes in ECs. To systemically identify targets and biological processes regulated by miR-181b, we comparatively analyzed the gene expression

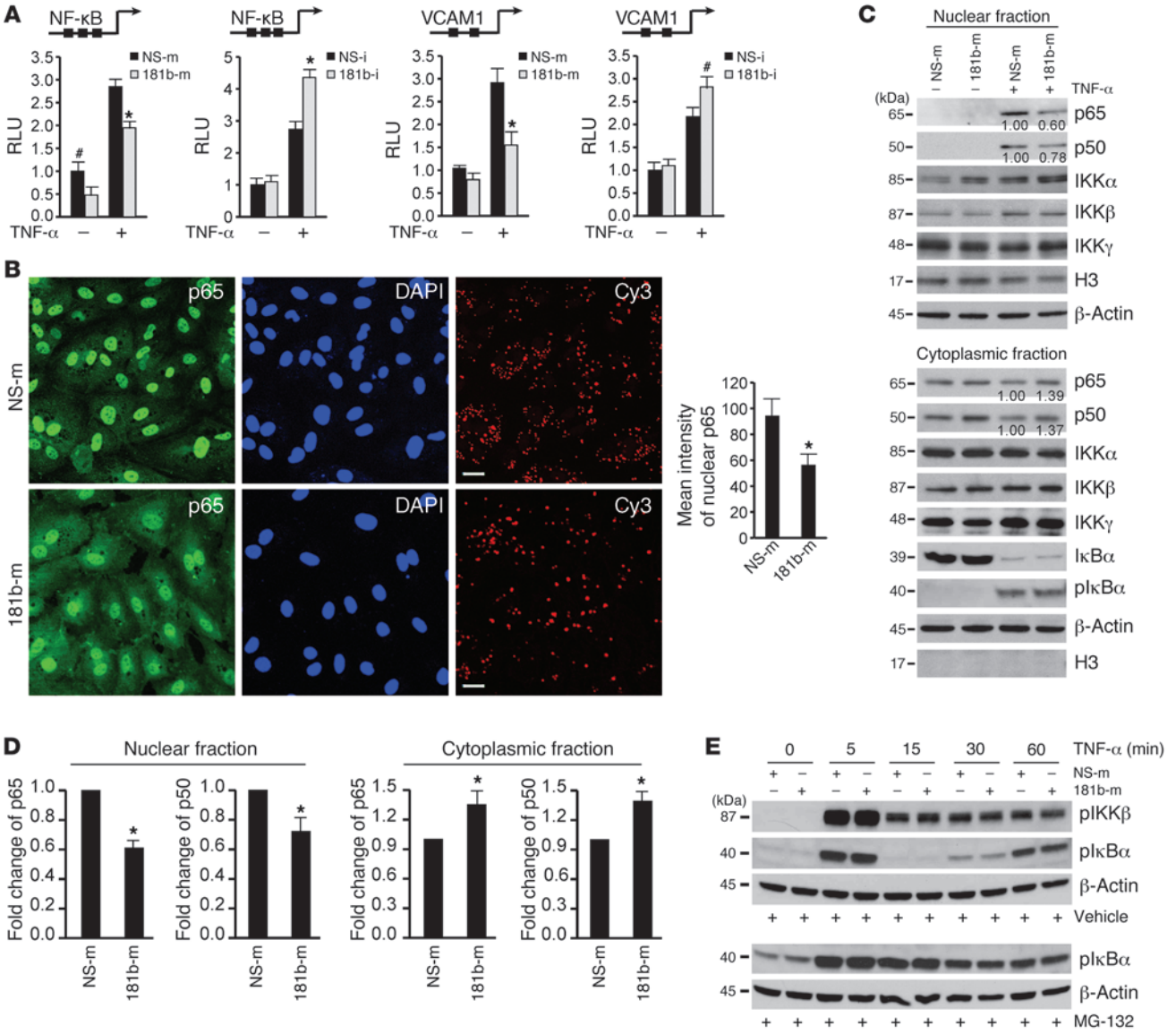

Figure 3

miR-181b inhibits the activation of the NF-κB signaling pathway. (**A**) Luciferase activity of reporters containing either the NF-κB concatemer or VCAM-1 promoter in HUVECs transfected with miRNA negative control or miR-181b mimics and miRNA inhibitor negative control or miR-181b inhibitor after 12 hours treatment with 10 ng/ml of TNF-α. $^{\#}P < 0.05$; $^{*}P < 0.01$. Values represent mean ± SD; $n = 3$. (**B**) p65 staining in HUVECs transfected with miRNA negative control or miR-181b mimics. Thirty-six hours after transfection, cells were treated with 10 ng/ml TNF-α for 60 minutes and processed for immunostaining with antibodies against p65. Cells were stained with DAPI to visualize the nucleus. Cy3-conjugated miRNA negative control was transfected at 3 nM concentration to show transfection efficiency in both groups. Images were acquired by confocal microscopy from 3 independent experiments, and values represent mean ± SD. $^{*}P < 0.01$. Scale bars: 20 μm. (**C**) The indicated proteins were detected in cytoplasmic or nuclear fractions prepared from HUVECs transfected with miRNA negative control or miR-181b mimics and treated with 10 ng/ml TNF-α for 1 hour. Densitometry was performed and fold change of p65 and p50 protein expression after normalization is shown below the corresponding band. Quantifications from 3 independent experiments were shown in **D**, and values represent mean ± SD. $^{*}P < 0.05$. (**E**) Western blot analysis of phosphorylated IκBα or IKKβ in HUVECs transfected with miRNA negative control, or miR-181b mimics and treated with 10 μM MG-132 or DMSO for 2 hours followed by 10 ng/ml TNF-α for the indicated times.

profiles of HUVECs transfected with miRNA negative control or miR-181b by using Agilent whole human genome microarrays. Transfected HUVECs were treated with TNF-α for 4 hours, and total RNA was isolated and processed for gene chip analysis. Out of the approximately 44,000 transcripts screened, we determined that 841 genes were downregulated and 928 genes were upregulated by at least 1.5-fold in miR-181b–overexpressing cells as compared with control cells. Over 200 of those genes are known to be NF-κB regulated. Moreover, of 24 selected genes known to be associated with inflammatory disease states, all were inhibited by overexpression of miR-181b. These reduced gene expression changes were verified by qPCR analysis (Figure 5,

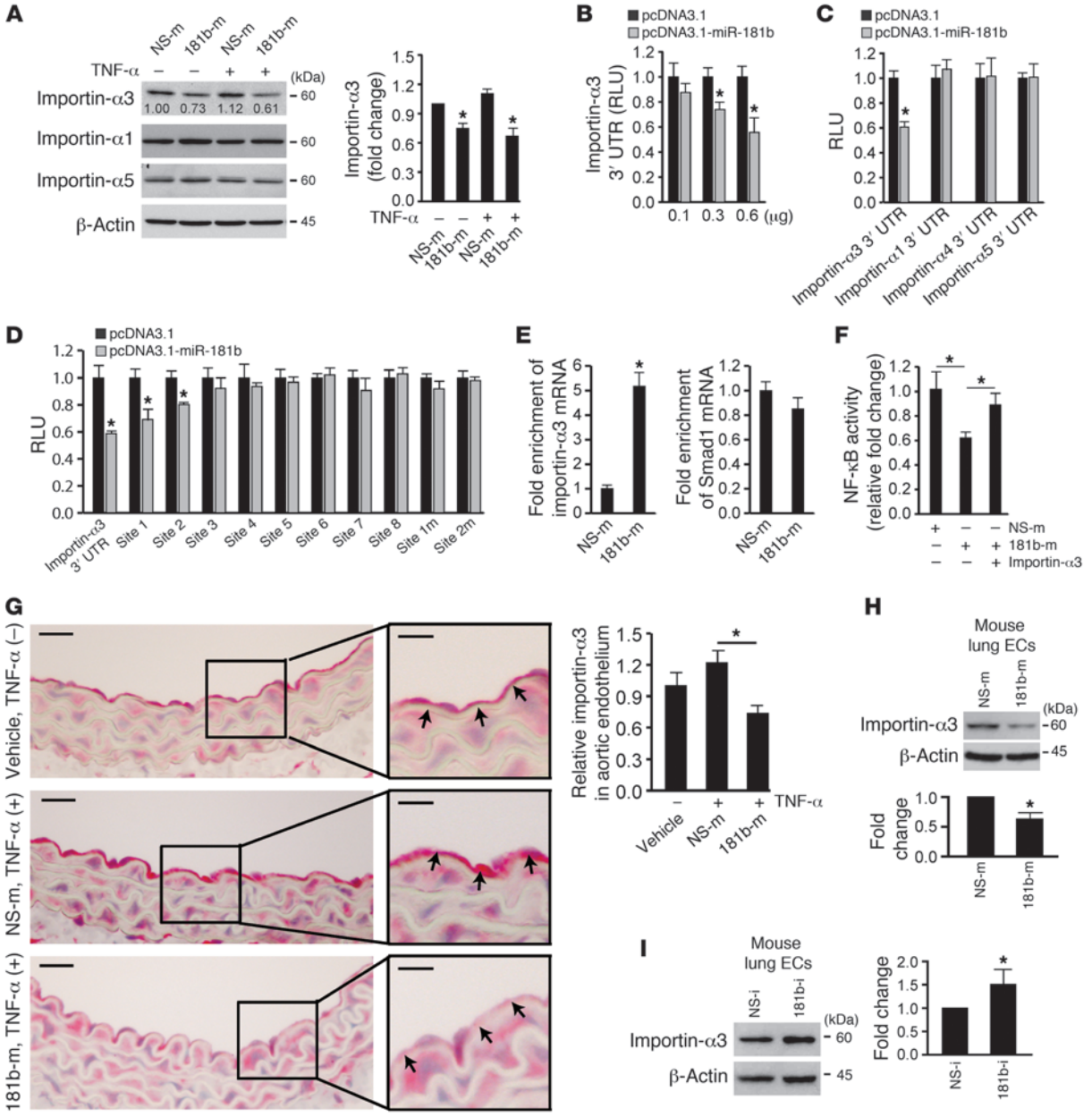

Figure 4

miR-181b reduces importin-α3 expression. (**A**) Western blot analysis of importin-α1, importin-α3, and importin-α5 in cells transfected with miRNA negative control or miR-181b mimics in the absence or presence of 10 ng/ml TNF-α. Mean ± SD, $n = 3$. *$P < 0.05$. (**B**) Normalized luciferase activity of a reporter containing the 3′ UTR of importin-α3 in cells cotransfected with increasing amounts of pcDNA3.1 empty vector or pcDNA3.1-miR-181b. *$P < 0.01$. (**C**) Normalized luciferase activity of a reporter containing the 3′ UTR of importin-α1, importin-α3, importin-α4, and importin-α5 cotransfected with either pcDNA3.1 empty vector or pcDNA3.1-miR-181b. *$P < 0.01$. (**D**) Normalized luciferase activity of a reporter containing 3′ UTR of importin-α3, predicted miR-181b–binding sites, or mutated miR-181b–binding sites. The reporter was cotransfected with either pcDNA3.1 empty vector or pcDNA3.1–miR-181b. *$P < 0.05$. (**E**) miRNP-IP analysis of enrichment of importin-α3 mRNA in HUVECs transfected with miRNA negative control or miR-181b mimics. *$P < 0.01$. (**F**) Luciferase activity of reporters containing the NF-κB concatemer in cells transfected with miRNA negative control or miR-181b mimics in the absence or presence of importin-α3 gene lacking its 3′ UTR. *$P < 0.05$. (**G**) Mice were i.v. injected with vehicle ($n = 3$ mice), miRNA negative control ($n = 4$ mice), or miR-181b mimics ($n = 5$ mice) and treated with TNF-α for 4 hours; aortas were harvested for importin-α3 staining. *$P < 0.05$. Scale bars: 20 μm (insets, 10 μm). (**H**) Western blot analysis of importin-α3 of lung ECs freshly isolated from mice treated with miRNA negative control or miR-181b mimics. Mean ± SD, $n = 3$. *$P < 0.05$. (**I**) Western blot analysis of importin-α3 of lung ECs freshly isolated from mice treated with miRNA inhibitor negative control or miR-181b inhibitor. Mean ± SD, $n = 3$. *$P < 0.05$.

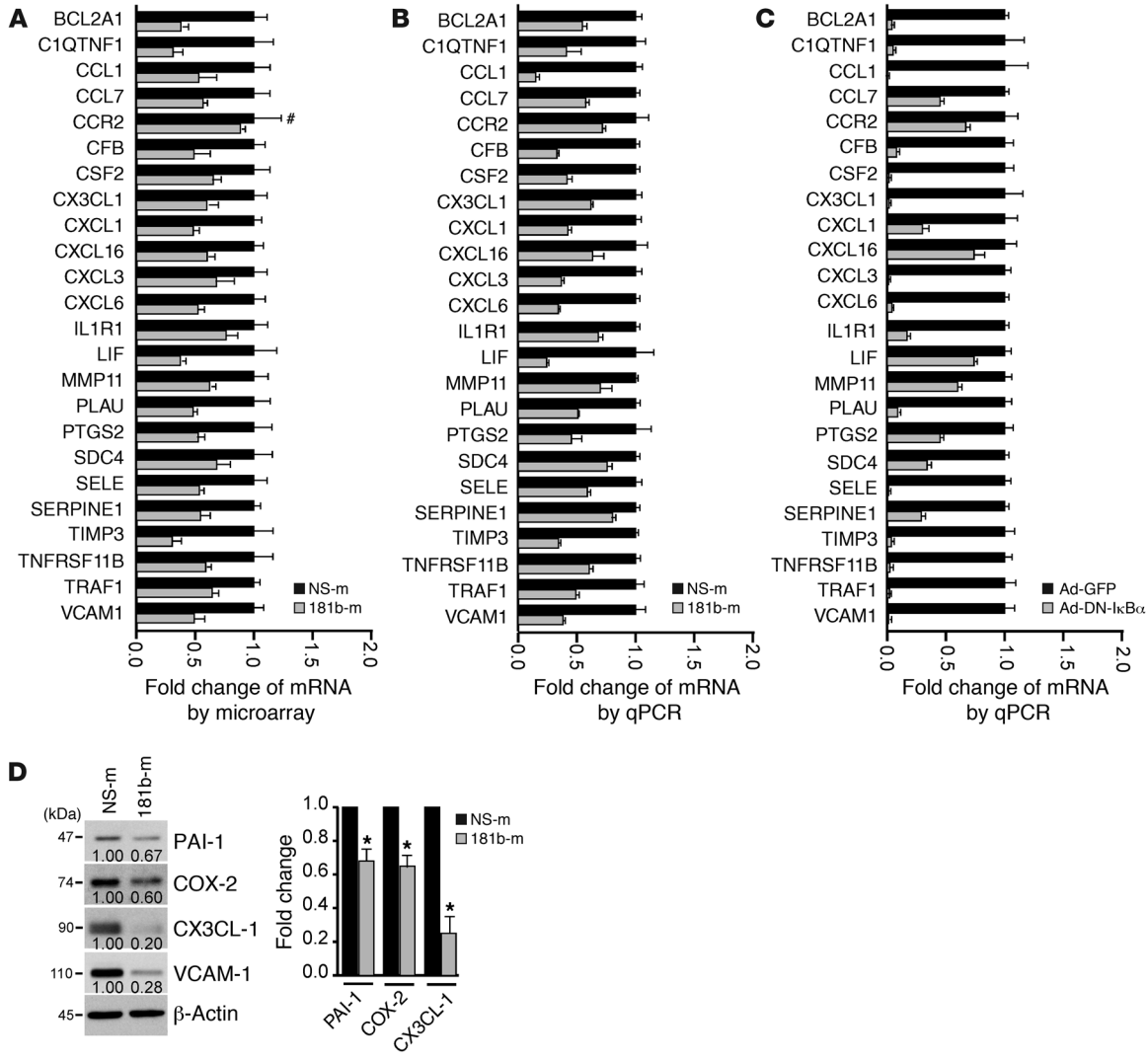

Figure 5

Gene expression profiling in HUVECs transfected with miR-181b and bioinformatics analysis. (**A**) Relative gene expression of 24 TNF-α–regulated genes in HUVECs transfected with miRNA negative control or miR-181b mimics, as identified by microarray gene chip assay. Expression is presented as fold change relative to HUVECs transfected with miRNA negative control. Data shown are mean ± SD, $n = 4$. #, nonsignificant comparison; all other genes examined were significantly reduced by miR-181b overexpression ($P < 0.05$). (**B**) Real-time qPCR analysis of the genes listed in **A**. All genes examined were significantly reduced by overexpression of miR-181b ($P < 0.05$). (**C**) HUVECs infected with control virus or Ad-DN-IκBα were treated with TNF-α and harvested for real-time qPCR analysis of the genes listed in **A**. All genes examined were significantly reduced by Ad-DN-IκBα ($P < 0.05$). (**D**) Western blot analysis of CX3CL-1, PAI-1 (gene symbol, SERPINE1), COX-2 (gene symbol, PTGS2), and VCAM-1 in HUVECs transfected with miRNA negative control or miR-181b mimics. Values represent mean ± SD, $n = 3$. *$P < 0.05$.

A and B). Because the dominant-negative IκBα is a specific inhibitor of the canonical NF-κB signaling, we examined the gene expression profile of the 24 selected genes by real-time qPCR in HUVECs transduced in the presence of an adenovirus expressing the dominant-negative IκBα. We found that the expression of each of the 24 genes was reduced by expression of the dominant-negative IκBα in response to TNF-α treatment (Figure 5C), revealing a similar profile to cells overexpressing miR-181b mimics (Figure 5B). PAI-1, COX-2, CX3CL-1, and VCAM-1 were chosen to verify concordant directional changes at the protein level in miR-181b–overexpressing ECs (Figure 5D). To identify highly regulated biological processes in miR-181b–overexpressing cells, we performed gene set enrichment analysis (GSEA), a computational method that determines whether a defined set of genes shows significant differences between 2 biological states (57). We found 6 enriched biological processes that were significantly represented by the reduced genes in miR-181b–overexpressing cells: response to cytokine stimulus; positive regulation of cell migration; regulation of inflammatory response; inflammatory response; chemotaxis; and IKK/NF-κB cascade (Table 1). An abundance of targets that interconnected with the NF-κB signaling pathway was also observed using the Ingenuity web-based pathway analysis program (Supplemental Figure 6). Taken together, these data suggest that miR-181b selectively suppresses an enriched set of NF-κB–regulated genes and components of inflammatory signaling pathways in response to TNF-α in ECs.

Table 1
Enriched GO biological processes downregulated in miR-181b overexpression cells, identified by GSEA at 25% FDR

GO biological processes	Description of gene set	FDR
GO:0034097	Response to cytokine stimulus	0.013
GO:0030335	Positive regulation of cell migration	0.171
GO:0050727	Regulation of inflammatory response	0.178
GO:0006954	Inflammatory response	0.194
GO:0006935	Chemotaxis	0.195
GO:0007249	IKK/NF-κB cascade	0.224

miR-181b reduces LPS-induced EC activation, leukocyte accumulation, lung inflammation/injury, and mortality. Sepsis is a medical condition with high morbidity and mortality and increasing incidence over the past few decades (58). The endotoxin LPS is a component of the outer membrane of Gram-negative bacteria that plays a significant role in the pathogenesis of about 25% to 30% of sepsis cases (59). LPS activates the TLR-mediated signaling pathway, induces the release of critical proinflammatory cytokines including TNF-α, and elicits a systemic inflammatory response syndrome (SIRS) (60, 61). During sepsis, activation of the vascular endothelium plays a critical role in the recruitment of neutrophils and monocytes/macrophages as well as subsequent exacerbation of the inflammatory response (1, 62). To determine whether miR-181b contributes to this process, we assessed whether the level of endothelial miR-181b could be affected in response to LPS and whether in vivo overexpression of miR-181b could reduce leukocyte recruitment and EC activation in a systemic LPS mouse model of vascular inflammation. As shown in Supplemental Figure 7A, the expression of miR-181b was reduced in freshly isolated aortic intima by 50% and 47% after 4 hours of systemic treatment with LPS or TNF-α, respectively. In contrast, *VCAM-1* mRNA was induced about 5.0-fold and 7.2-fold by TNF-α and LPS, respectively, in freshly isolated aortic intima (Supplemental Figure 7B). In vivo i.v. administration of miR-181b mimics reduced the induction of VCAM-1 expression in response to LPS by 60% (Figure 6, A and E). Analysis of lung sections taken from mice injected with miR-181b revealed a significant reduction of CD45-positive (common leukocyte antigen) and Gr-1–positive (predominantly neutrophil) leukocytes (by 54% and 58%, respectively) in response to LPS treatment (Figure 6, A, C, and D). Importantly, the number of Gr-1–positive leukocytes adherent to the pulmonary vascular endothelium was reduced 47% by miR-181b overexpression (Figure 6, G and H). We also observed reduced interstitial edema and lung injury scores in the lungs of mice in which miR-181b was overexpressed (Figure 6, A and B). Myeloperoxidase activity, reflecting the presence of peroxidase enzyme expressed most abundantly in neutrophils, was also reduced by miR-181b overexpression (Figure 6F). Finally, systemic delivery of miR-181b mimics in mice (2 injections before and 1 injection after the initiation of LPS-induced endotoxic shock) reduced mortality from endotoxemia by 75% over 4 days (Figure 6I). Taken together, these results demonstrate a critical role for miR-181b in endotoxin-induced endothelial activation and leukocyte accumulation and suggest that overexpression of miR-181b could represent a novel class of therapeutic avenues for limiting endotoxin-induced vascular inflammation and may ultimately have a beneficial effect in critical illness.

miR-181b inhibits the activation of the NF-κB pathway in vascular endothelium in vivo. In response to inflammatory stimuli, activation of the NF-κB pathway, which involves translocation of NF-κB heterodimers from cytoplasm to nucleus, is critical for vascular inflammation in vivo (24, 26). To determine whether miR-181b regulates NF-κB translocation in vivo, miR-181b was systemically administered by tail-vein injection, and mice were challenged with or without LPS. In mice not exposed to LPS, the majority of NF-κB p65 remained cytoplasmic in pulmonary ECs (Figure 7A). In contrast, NF-κB p65 colocalized more with DAPI-stained endothelial nuclei by immunofluorescence in mice challenged with LPS by i.p. injection (Figure 7A). Remarkably, the accumulation of NF-κB p65 in endothelial nuclei in response to LPS was reduced by 45% in the presence of systemically delivered miR-181b compared with mice injected with NS control miRNA (Figure 7A). Using a complementary approach, we also analyzed the effect of miR-181b on NF-κB activation in vivo in NF-κB transgenic mice, which express a luciferase reporter driven by an NF-κB–responsive promoter (63, 64). Indeed, systemic delivery of miR-181b reduced LPS-induced luciferase activity in lungs by 57% (Figure 7B), NF-κB target genes VCAM-1 and E-selectin in lungs by 43% and 59%, respectively (Figure 7, C and D), and VCAM-1 expression in isolated mouse lung ECs by 52% (Figure 7E). These effects were associated with approximately 4.5-fold overexpression of miR-181b in the lungs by real-time qPCR compared with mice injected with NS control miRNA (Figure 7F). Importantly, miR-181b reduced LPS-induced luciferase to a degree similar to that of adenoviral vectors expressing a dominant-negative IκBα, and no additional inhibitory effect of miR-181b was observed when delivered in combination with adenoviral vectors expressing a dominant-negative IκBα (Figure 7G). Finally, miR-181b overexpression had no effect on the expression of a panel of miRNAs in mouse lungs, which have been shown to regulate inflammatory genes or NF-κB activation, including miR-10a, miR-146a, miR-155, miR-31, and miR-17-3p (Supplemental Figure 8). These data suggest that systemic delivery of miR-181b inhibits endothelial NF-κB p65 nuclear translocation and, subsequently, the activation of NF-κB signaling pathway in vascular ECs in vivo.

Inhibition of miR-181b potentiated LPS-induced NF-κB–regulated gene expression and NF-κB activity in vivo. To determine whether the endogenous expression of miR-181b has any effect on NF-κB signaling and EC activation in vivo, mice were injected i.v. with miR-181b inhibitors in the presence of LPS. As shown in Figure 8, A and B, systemic delivery of miR-181b inhibitors reduced endogenous miR-181b expression by approximately 62% and potentiated LPS-induced VCAM-1 protein expression by approximately 1.9-fold in lung tissues. The expression of *VCAM-1* and *E-selectin* mRNA also increased by approximately 1.9- and 1.5-fold, respectively (Figure 8, C and D). Furthermore, miR-181b inhibition enhanced NF-κB activity in lung lysates from NF-κB–luciferase transgenic mice treated with LPS (Figure 8E) and exacerbated lung injury, as shown by scoring (Figure 8G). Finally, in response to LPS, leukocyte accumulation in the lungs of mice treated with miR-181b inhibitors was markedly increased by immunohistochemistry studies compared with that in mice treated with NS control inhibitors (Figure 8, F, H, and I). These findings indicate that inhibition of endogenous miR-181b potentiates NF-κB signaling, EC activation, and lung inflammation in the presence of inflammatory stimuli, suggesting that reduced miR-181b expression may play a role in the pathogenesis of sepsis.

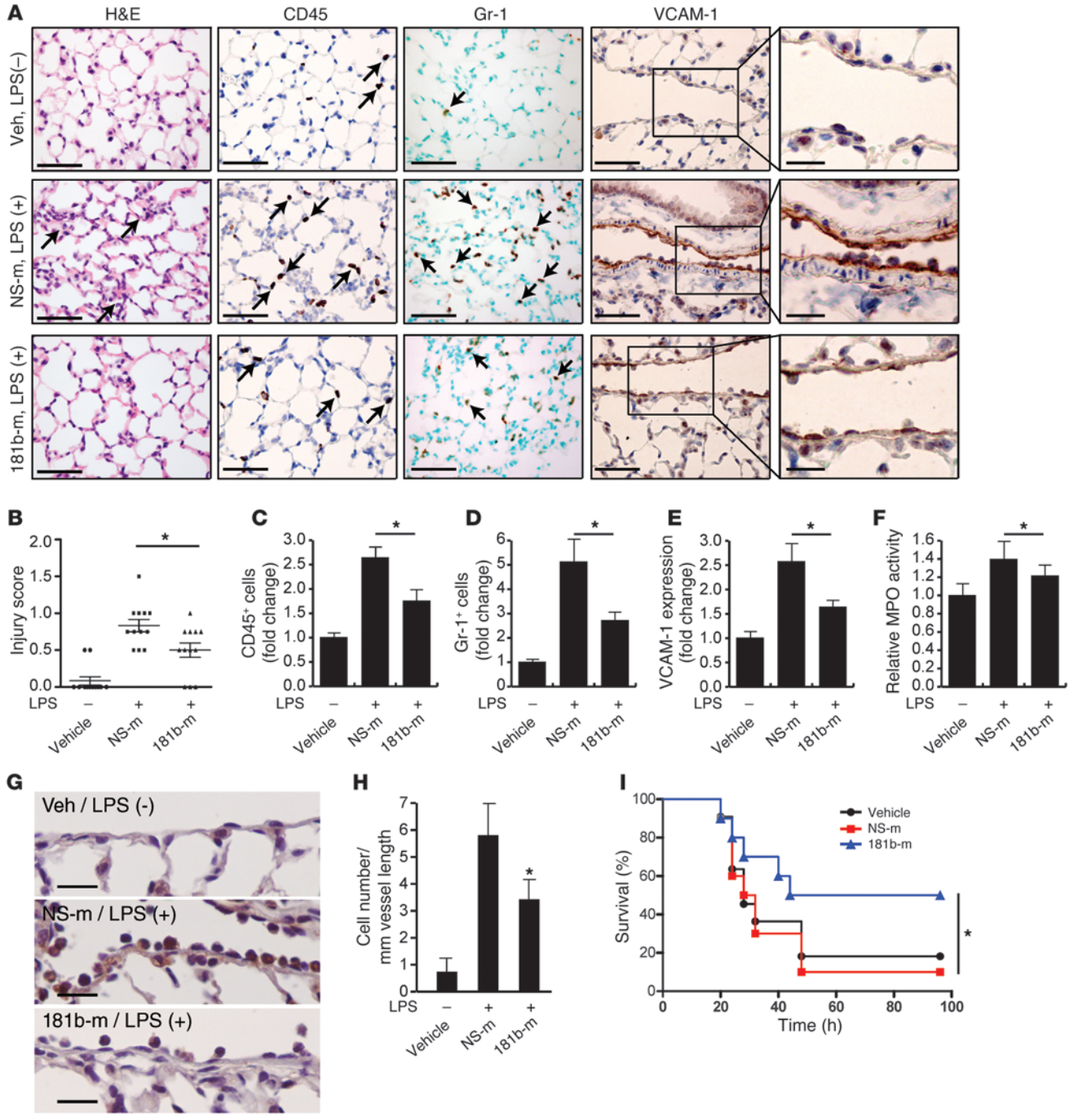

Figure 6

miR-181b reduces EC activation and leukocyte accumulation in LPS-induced lung inflammation/injury. (**A**) Mice were i.v. injected with vehicle, miRNA negative control, or miR-181b mimics and treated with or without LPS (40 mg/kg, i.p., serotype 026:B6) for 4 hours; lungs were harvested and stained for H&E, Gr-1, CD45, or VCAM-1 staining. Scale bars: 50 μm (insets, 20 μm). (**B**) Evaluation of lung injury 4 hours after LPS was determined by lung injury scoring. Each data point represents score from 1 section. $n = 4$ mice per group, and 3 sections per mouse were scored. *$P < 0.05$. (**C**) Quantification of CD45-positive cells. *$P < 0.05$. (**D**) Quantification of Gr-1 positive cells. *$P < 0.05$. (**E**) Quantification of VCAM-1 expression. *$P < 0.05$. $n = 4$ mice per group; values represent mean ± SD (**C**–**E**). (**F**) Mice were treated as in **A**. Lungs were harvested and assessed for MPO activity, and the value of the vehicle group was set to 1. Values represent mean ± SD, $n = 6$ mice per group. (**G** and **H**) Mice were treated as in **A**, and lungs were harvested for Gr-1 staining. Scale bars: 20 μm. Quantification shows the number of Gr-1–positive cells per mm vessel length. Values represent mean ± SD, $n = 4$. *$P < 0.05$. (**I**) Kaplan-Meier survival curves of: LPS-treated C57BL/6 mice (50 mg per kg, i.p., $n = 10$ to 11 per group) that were injected i.v. with vehicle (black circles), miRNA negative control (red squares), or miR-181b mimics (blue triangles) 48 hours before, 24 hours before, and 1.5 hours after LPS administration. *$P < 0.05$, 1-tailed log-rank test.

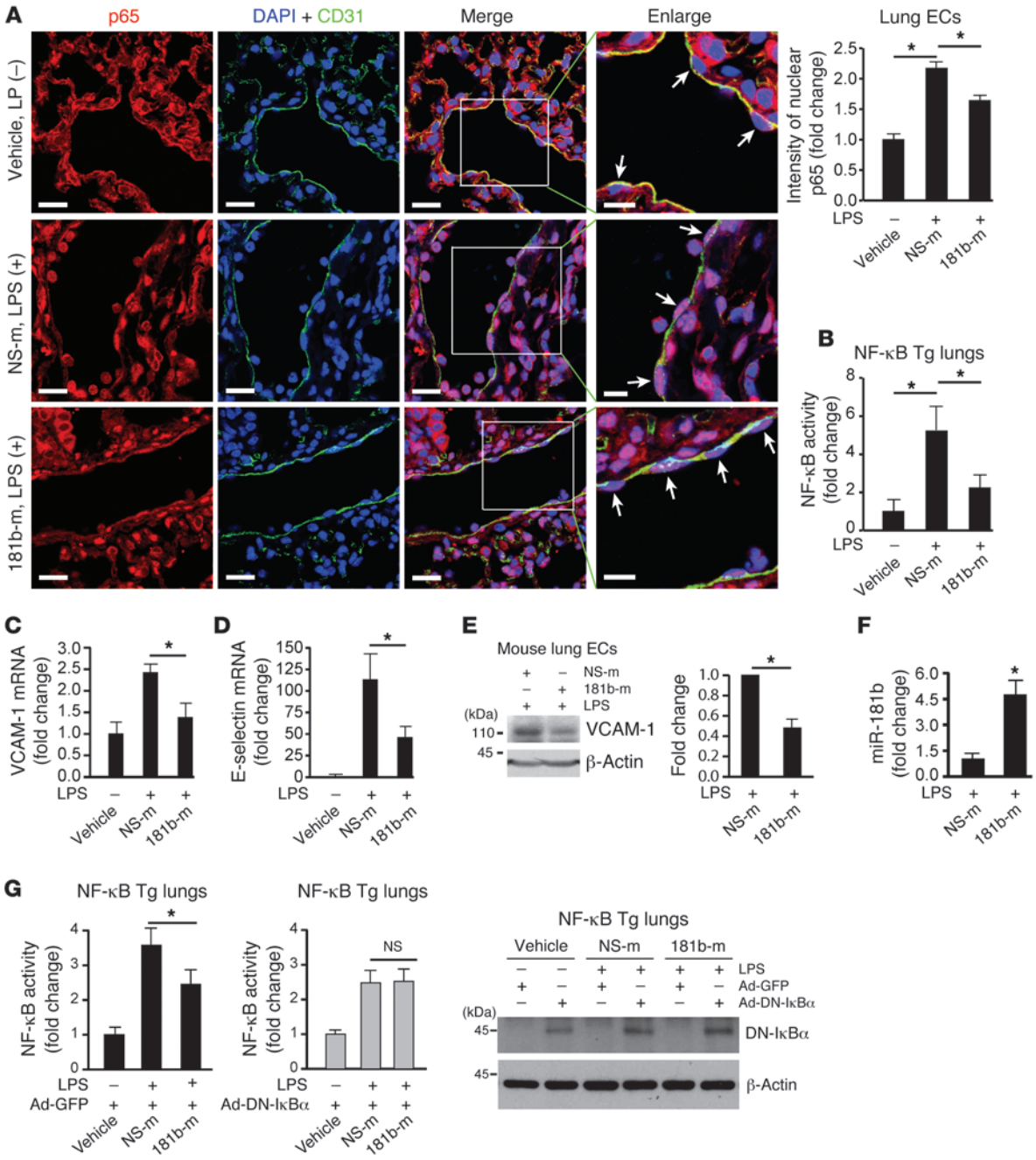

Figure 7

Systemic delivery of miR-181b inhibits NF-κB activation in vivo. (**A**) Mice (n = 3–5 per group) were injected with vehicle, miRNA negative control, or miR-181b 3 times, and lungs were harvested on day 4 after 2 hours of 10 mg/kg LPS (026:B6, i.p.) for immunostaining with anti-p65 (red), anti-CD31 (green), and DAPI (blue). Arrows indicate differential p65 accumulation in nuclei of ECs after treatment. Scale bars: 20 μm (insets, 10 μm). Nuclear p65 was quantified in vascular ECs reflecting vehicle (n = 22 ECs), miRNA negative control (n = 40 ECs), and miR-181b mimics (n = 39 ECs). Mean ± SEM. *P < 0.01. (**B**) NF-κB luciferase transgenic mice (n = 4 per group) were injected with vehicle, miRNA negative control, or miR-181b as described in **A**. On day 4, 4 hours after 10 mg/kg LPS (026:B6), lungs were harvested for luciferase activity assay. Mean ± SD. *P < 0.05. (**C** and **D**) Real-time qPCR analysis of VCAM-1 or E-selectin. Mean ± SEM. *P < 0.05. (**E**) Western blot analysis of VCAM-1 in freshly isolated lung ECs from treated mice. Mean ± SEM, n = 2. *P < 0.05. (**F**) Real-time qPCR analysis of miR-181b expression in lungs after 4 hours LPS. Mean ± SD. *P < 0.01. (**G**) NF-κB luciferase transgenic mice (n = 6–8 per group) were injected with recombinant adenovirus Ad-GFP or Ad–DN-IκBα, followed by i.v. injection of vehicle, miRNA negative control, or miR-181b as described in **A**. Lungs were harvested on day 5 after 4 hours of 10 mg/kg LPS (026:B6) for luciferase activity assay and Western blot analysis. Mean ± SD. * P < 0.05.

Circulating levels of miR-181b are reduced in patients with sepsis. Accumulating studies have reported that miRNA can be detected in the plasma and other body fluids (65–67). To examine the regulation of circulating miR-181b in an acute inflammatory disease, we determined the levels of miR-181b in plasma from patients with sepsis or with sepsis and acute respiratory distress syndrome (ARDS). As shown in Figure 9, A and B, the levels of circulating miR-181b were reduced by approximately 40% in patients with sepsis or sepsis plus sepsis/ARDS compared with control subjects admitted to the intensive care unit (ICU) without sepsis. In a multivariate logistic regression model adjusting for the Acute Physiology and Chronic Health Evaluation II (APACHE II) score, a classification system to reflect the severity of disease upon admission to an ICU in the hospital (68), the miR-181b level was independently associated with sepsis (odds ratio [OR] 0.49, 95% CI 0.25–0.95, $P = 0.03$) and sepsis plus sepsis/ARDS (OR 0.52, 95% CI 0.29–0.92, $P = 0.03$). Thus, after adjusting for APACHE II score, each one unit increase in miR-181b level was associated with an approximately 50% decrease in the odds of having sepsis. The characteristics of control subjects and septic patients are shown in Table 2. Collectively, these data indicate that reduced circulating miR-181b levels in the plasma are associated with patients with sepsis.

Discussion

Sustained EC activation may adversely contribute to the pathogenesis of both acute and chronic inflammatory disease states. Herein, we provide evidence that miR-181b is dynamically regulated in response to proinflammatory stimuli and functions to suppress the expression of an enriched set of NF-κB target genes associated with inflammatory disease states, such as adhesion molecules (e.g., VCAM-1, E-selectin), chemokines and chemokine receptors (e.g., CCL1, CCL7, CX3CL1, CXCL1, CCR2), and other key inflammatory mediators (e.g., COX-2, PAI-1). In support, using complementary gain- and loss-of-function approaches, we demonstrated that miR-181b inhibits downstream NF-κB signaling by directly targeting importin-α3 in vitro and in vivo, an effect that inhibits nuclear accumulation of p50 and p65, and reduced expression of adhesion molecules, leukocyte accumulation, and vascular inflammation in vivo. Importantly, systemic delivery of miR-181b inhibited activation of the NF-κB pathway and reduced mortality of endotoxemic mice by reducing NF-κB nuclear translocation. Moreover, systemic overexpression of a dominant-negative IκBα completely blocked the inhibitory effect of miR-181b on LPS-induced NF-κB activation in the lungs. In light of these findings, these studies identify miR-181b as a novel regulator of EC activation and downstream NF-κB signaling in vitro and in vivo.

ECs perform multiple functions that are critical to vascular homeostasis, including controlling leukocyte trafficking, regulating vessel wall permeability, and maintaining blood fluidity. The recruitment of leukocytes and extravasation into the blood vessel wall are essential early events in normal inflammatory responses and related disease states (9, 69–71). Our findings that miR-181b can potently inhibit adhesion molecules, chemokines, and other NF-κB–responsive mediators suggest that it may serve to dampen the early stages of vascular inflammation. Furthermore, miR-181b–mediated inhibition of NF-κB targets was observed for several major physiologic proinflammatory mediators, such as TNF-α and LPS (Figures 1, 2, 5, and 6). Remarkably, miR-181b expression was also rapidly reduced in response to these stimuli in vitro and in vivo, an effect that may allow for enhanced NF-κB signaling. Consistent with this hypothesis, use of miR-181b inhibitors increased (a) leukocyte adhesion to stimulated EC monolayers; (b) leukocyte accumulation and lung injury scores; (c) NF-κB activity in lung lysates; and (d) expression of NF-κB target genes (*VCAM-1* and *E-selectin*) in vivo (Figure 1F and Figure 8). The effect of miR-181b was determined to be specific for the NF-κB signaling pathway, as the majority of the TNF-α–inducible genes examined were inhibited by miR-181b and were "phenocopied" by overexpression of a dominant-negative IκBα (Figure 5). Moreover, interrogation of the entire set of over 800 miR-181b–reduced genes identified by microarray analysis revealed 6 biological signaling pathways associated with NF-κB activation. In addition, miR-181b had no inhibitory effect on phosphorylation of the MAPK downstream mediators, ERK, p38, and JNK (Supplemental Figure 3B). Interestingly, in the presence of LPS, systemic delivery of miR-181b mimics failed to inhibit NF-κB–regulated targets COX-2 and IL-1β and NF-κB activity in PBMCs (Supplemental Figure 9). These findings indicate that the maintenance of miR-181b expression in the vascular endothelium is a key feature in controlling NF-κB signaling events and vascular inflammation.

miR-181b belongs to the miR-181 family, which consists of 4 members, miR-181a, miR-181b, miR-181c, and miR-181d. The biological functions of this miRNA family were first identified when miR-181a was recognized as a contributor to hematopoietic lineage commitment and differentiation (72, 73). Later studies revealed that increased miR-181a activity in primary embryonic lymphatic ECs resulted in substantially reduced levels of *Prox1* mRNA and protein and, consequently, regulated vascular development and neo-lymphangiogenesis (74). miR-181b was defined as a regulator of the B cell primary antibody repertoire based upon its ability to restrict the activity of activation-induced cytidine deaminase (75). Altered expression levels of both miR-181a and miR-181b have been detected in multiple tumors and leukemia/lymphoma (76–85), raising the intriguing possibility that dysregulation of NF-κB signaling in these cancers may be associated with defective miR-181 expression and/or function. Indeed, reduced expression of miR-181b has been observed in several primary human cancers, including astrocytic tumors, gastric, lung, and prostate cancer, glioma cells, acute myeloid leukemia, and chronic lymphocytic leukemia (76–86), an effect associated with a poor prognosis in several cancer subtypes (77–82, 86). In contrast, miR-181b has been found overexpressed in some cancers (87–89). For example, a recent study identified CYLD as a target of miR-181b-1 in an Src-transformed mammary epithelial cell line, an effect that potentiated NF-κB expression (88). A number of important differences exist between this study and ours, including the following: (a) cell type–specific differences — transformed (MCF-10A) cells versus primary ECs; (b) use of different stimuli — Src-oncoprotein increased versus cytokine/LPS decreased miR-181b expression; and (c) cell type–specific effects on *CYLD* gene expression — we observed no significant effect of miR-181b on CYLD expression in HUVECs (Supplemental Figure 10). The use of miR-181b, as well as other microRNAs, for therapeutic purposes will require careful scrutiny as this nascent field progresses. Finally, members of the miR-181 family may have nonredundant functions, as was suggested by evidence of one study in which miR-181a, but not miR-181c, promoted CD4 and CD8 double-positive T cell development when ectopically expressed in thymic progenitor cells (90). In the present study, we found that miR-181b is the dominant miR-181 family member expressed in ECs

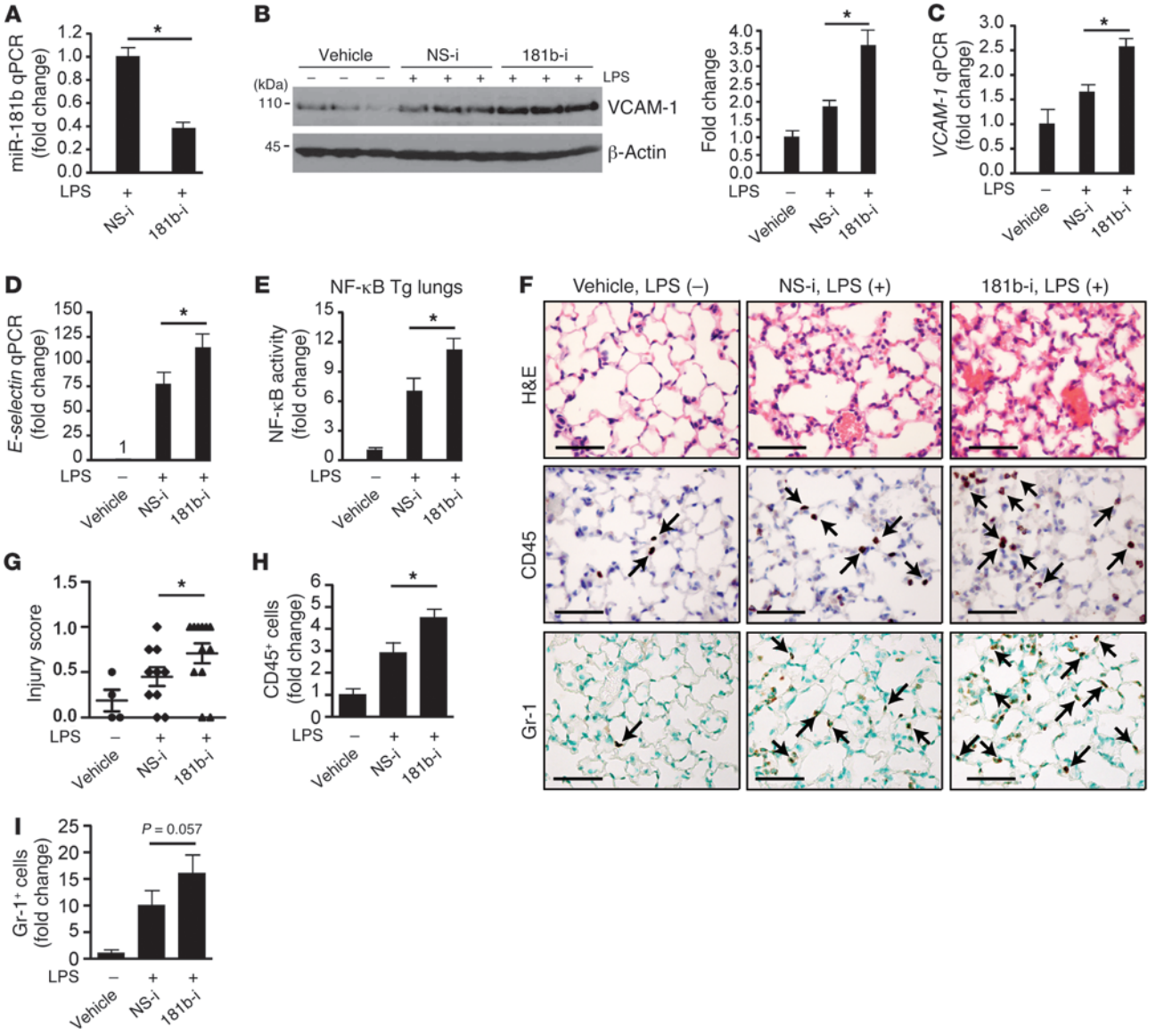

Figure 8

Inhibition of miR-181b potentiates LPS-induced proinflammatory gene expression in vivo. (**A**–**E**) NF-κB transgenic mice ($n = 5$ per condition) were i.v. injected with vehicle, miRNA inhibitor negative control, or miR-181b inhibitors (2 nmol/injection, 3 injections on consecutive days). Twenty-four hours after the last injection, mice were treated with or without LPS (10 mg/kg) for 4 hours, and lungs were harvested for different assays. (**A**) Real-time qPCR analysis of miR-181b expression. Mean ± SEM. (**B**) Western blot analysis of VCAM-1 protein expression. Densitometry was performed, and fold change of protein expression was quantified. Mean ± SEM. (**C**) Real-time qPCR analysis of *VCAM-1* mRNA expression. Mean ± SEM. (**D**) Real-time qPCR analysis of *E-selectin* mRNA expression. Mean ± SEM. (**E**) Luciferase activity in lung lysates. Mean ± SD. (**F**–**I**) Mice ($n = 3$–5 per group) were treated as in **A**. (**F**) H&E, CD45, Gr-1 staining of lung sections. Scale bars: 50 μm. (**G**) Evaluation of lung injury 4 hours after LPS was determined by lung injury scoring. Each data point represents a score from 1 section. 2 or 3 sections per mouse were scored. (**H**) Quantification of CD45-positive cells. Mean ± SD. $^*P < 0.05$. (**I**) Quantification of Gr-1–positive cells. Mean ± SD.

and is capable of potently suppressing EC activation by targeting importin-α3 in vitro and in vivo.

The role of miRNAs in ECs related to inflammatory and immune responses has only recently begun to emerge. miR-126, an EC-enriched miRNA, was found to regulate endothelial expression of VCAM-1 by directly targeting its 3′ UTR (91). A more recent microarray-based study showed that miR-31 and miR-17-3p are inducible by TNF-α and target the 3′ UTRs of E-selectin and ICAM-1, respectively, to reduce their expression (35). The above 2 studies suggest miRNAs can reduce proinflammatory gene expression in ECs by targeting the 3′ UTR of these genes. Recently, an antiinflammatory role was demonstrated for miR-10a in ECs (34). The expression of endothelial miR-10a was lower in the atherosusceptible regions of the aortic arch than in the nearby regions of the descending thoracic aorta (34). miR-10a was reported to inhibit NF-κB–mediated EC activation in vitro by reducing the expression of mitogen-activated kinase kinase kinase 7 and β-transducin repeat-containing gene, 2 key regulators of TNF-α degradation;

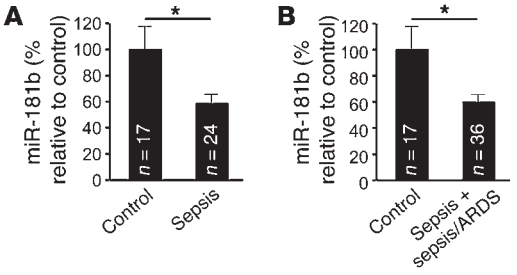

Figure 9
Circulating miR-181b levels are reduced in plasma from patients with sepsis or sepsis/ARDS. (**A**) Circulating miR-181b in either patients with sepsis (n = 26) or control subjects admitted to the ICU without sepsis (n = 16). (**B**) Circulating miR-181b in patients with sepsis plus sepsis/ARDS (n = 36) compared with control subjects (n = 16). The expression levels of miR-181b were detected by real-time qPCR. Data show mean ± SEM. *P < 0.05.

furthermore, an inverse association was observed between the expression of miR-10a and mitogen-activated kinase kinase kinase 7, β-transducin repeat-containing gene, and nuclear p65 (34). Thus, in response to inflammatory stimuli, the expression of several miRNAs would be expected to be differentially regulated in a spatial and temporal manner to fine-tune the output of the NF-κB signaling pathway via multiple upstream, downstream, and feedback regulatory mechanisms. While some miRNAs have been reported to directly alter the expression of other miRNAs in pathophysiological states, we found no effect of systemically delivered miR-181b in vivo on the expression of any of the miRNAs implicated in affecting NF-κB activation, including the following: miR-10a (targets mitogen-activated kinase kinase kinase 7 [MAP3K7; TAK1] and β-transducin repeat-containing gene [β-TRC]), miR-146a (targets TNF receptor-associated factor 6 [TRAF6] and IL-1 receptor-associated kinase 1 [IRAK1]), miR-155 (targets IKKβ and IKKε), miR-31 (targets E-selectin), and miR-17-3p (targets ICAM-1) (Supplemental Figure 8). Considering these findings, we have identified an unexpected role for miR-181b in its unique ability to inhibit downstream NF-κB nuclear translocation via targeting importin-α3, an effect that is distinct from that of other miRs that have been implicated in regulating upstream NF-κB signals.

Importins are a family of proteins involved in nuclear translocation. We demonstrate by a combination of experimental approaches, including bioinformatics, 3′ UTR reporter assays, miRNP-IP, and in vivo expression and functional analyses, that importin-α3 is necessary and sufficient to mediate miR-181b's inhibitory effect on NF-κB and NF-κB–responsive gene expression in response to proinflammatory stimuli. Indeed, overexpression of importin-α3 (lacking its 3′ UTR) effectively rescued miR-181b–mediated inhibition of NF-κB–induced activity in vitro and in vivo (Figure 4F and Supplemental Figure 5I). Conversely, siRNA knockdown of importin-α3 "phenocopied" miR-181b's inhibitory effects on NF-κB activity and targets (VCAM-1 and E-selectin) in vitro and in vivo (Supplemental Figure 5, A–G). Importin-α3 has been previously implicated in regulating nuclear translocation of p50 and p65 in other cell systems; for example, alteration of importin-α3 expression is the mechanism by which prohibitin reduces NF-κB activation in intestinal epithelial cells (92). Because we did not observe any effect of miR-181b on IKK complex proteins or IκBα phosphorylation (Figure 3, C–E, and Supplemental Figure 3A), miR-181b–mediated inhibitory effects are not likely to be associated with these upstream events. Indeed, multiple prediction databases did not reveal miR-181b–binding sites in the 3′ UTRs of IκBα, IKKα, IKKβ, or IKKγ. In addition, while miR-181b inhibits the expression of upstream receptors implicated in NF-κB signaling, such as TRAF1, TNFRSF11B, and IL1R1 (Figure 5), we found that miR-181b could not inhibit the 3′ UTRs for these genes (Supplemental Figure 4D). Indeed, these genes are known to be NF-κB responsive (93–95).

Accumulating studies have implicated circulating miRNAs in acute inflammatory diseases such as sepsis, a life-threatening condition associated with poor outcome. We identified patients with sepsis or sepsis plus sepsis/ARDS as having reduced circulating plasma levels for miR-181b compared with control patients admitted to the ICU without sepsis (Figure 9). Furthermore, after adjusting for the APACHE II score (a measure of severity of disease at presentation to the ICU), miR-181b was independently associated with sepsis or sepsis plus sepsis/ARDS. These findings coupled with the improved survival observed in miR-181b "rescue" studies in septic mice (Figure 6I) suggest that therapies directed at restoring miR-181b expression may ameliorate this acute inflammatory process. To date, 3 other miRNAs have been identified in plasma as potential biomarkers for sepsis patients. miR-150, initially identified from leukocyte profiling, was also reduced in plasma of sepsis patients and correlated with increasing severity of Sequential Organ Failure Assessment (SOFA) score (96). Circulating levels of miR-146a and miR-223 were also found reduced in sepsis patients compared with patients with SIRS or healthy controls (97). Collectively, these findings indicate that miRNAs correlate with varying levels of severity of sepsis for patients admitted to the ICU.

In summary, we have identified miR-181b as a cytokine-responsive miRNA that regulates the expression of key NF-κB–regulated genes involved in the endothelial response to inflammation in vitro and in vivo by regulating the NF-κB signaling pathway. These findings also revealed an unexpected mechanistic role for this miRNA in targeting downstream NF-κB signaling by directly targeting importin-α3. These studies support the possibility that miR-181b may serve as an important "inflamiR" by controlling critical aspects of EC homeostasis under physiologic or pathologic conditions. Strategies aimed at restoring miR-181b expression may provide a novel therapeutic approach to limiting acute inflammatory disease states.

Methods

Reagents. InSolution MG-132 (no. 474791) was from Calbiochem. Cy3 dye–labeled Pre-miR Negative Control #1 (AM17120), Pre-miR miRNA

Table 2
The characteristics of control subjects and septic patients

	Control subjects (n = 17)	Sepsis (n = 24)	Sepsis plus sepsis/ARDS (n = 36)
Age (years)	65.2 ± 16.2	54.3 ± 15.8	53.2 ± 14.5
Male/female	7/10	16/8	21/15
APACHE II score	20.3 ± 6.6	24.9 ± 9.2	26.2 ± 9.2
28-day mortality (%)	17.7%	20.8%	27.8%

Age and APACHE II score are shown in mean ± SD.

Precursor Molecules Negative Control #1 (AM17110), Pre-miR miRNA Precursor Molecules miR-181b (PM12442), Anti-miR miRNA Inhibitors Negative Control #1 (AM17010), and miR-181b Inhibitor (AM12442) were from Ambion. For in vivo studies, oligomers with the same sequences were synthesized on a larger scale. For more information, see Supplemental Methods.

Cell culture, transfection, and adenoviral transduction. THP-1 cells were from ATCC and cultured in ATCC-formulated RPMI 1640 medium (no. 30-2001) supplemented with 10% fetal bovine serum and 0.05 mM 2-mercaptoethanol. HUVECs were obtained from Lonza (cc-2159) and cultured in EC growth medium EGM-2 (cc-3162). Cells passaged less than 5 times were used for all experiments. Lipofectamine 2000 transfection reagent from Invitrogen was used for transfection, following the manufacturer's instructions. miRNA negative control or miR-181b mimics were transfected at 10 nM concentration, and miRNA inhibitor negative control or miR-181b inhibitor were transfected at 50 nM except where indicated. Cells were allowed to grow for 36 hours before treatment of 10 ng/ml recombinant human TNF-α from R&D Systems (210-TA/CF) for various times, according to the experiment: Western blot, 8 hours; real-time qPCR, 1, 4, 8, or 24 hours; and ELISA, 16 hours. HUVECs were transduced with recombinant adenoviruses, Ad-GFP, or Ad-DN-IκBα (expressing dominant negative IκBα) at 100 PFU. For reporter studies, HUVECs were plated (50,000/well) in triplicate on a 12-well plate, grown to 70%–80% confluency, and transfected with 200 ng of the indicated reporter constructs and 100 ng β-gal expression plasmids. miR-181b mimics or inhibitors were cotransfected at 10 or 50 nM final concentration where indicated; after 36 hours of incubation, cells were treated with 10 ng/ml TNF-α for 8 hours. In some experiments, pcDNA3.1–miR-181b or empty vector was cotransfected with 200 ng reporter constructs and 100 ng β-gal expression plasmids. For rescue studies, NF-κB concatemer luciferase reporter was cotransfected with pcDNA3.1–miR-181b or empty vector in the presence or absence of open reading frame cDNA of importin-α3 into 293T cells. Transfected cells were collected in 200 μl Reporter Lysis Buffer (Promega). The activity of luciferase and β-gal was measured. Each reading of luciferase activity was normalized to the β-gal activity read for the same lysate.

Cell adhesion assay. HUVECs grown in 12-well plates were transfected with miRNA mimics or inhibitors. Twenty-four hours later, transfected cells were replated onto 96-well fluorescence plates (353948; BD) for overnight growth. The following day, 10 ng/ml TNF-α was added for 5 hours. THP-1 cells (ATCC) were washed with serum-free RPMI 1640 medium and suspended at 5×10^6 cells/ml in medium with 5 μM of Calcein AM (C3100MP; Invitrogen). Cells were kept in an incubator containing 5% CO_2 at 37°C for 30 minutes. The labeling reaction was stopped by the addition of the cell growth medium, and cells were washed with growth medium twice and resuspended in growth medium at 5×10^5 cells/ml. After 5 hours of TNF-α treatment, HUVECs were washed once with THP-1 cell growth medium, and 200 μl Calcein AM–loaded THP-1 cells were added to each well. After 1 hour of incubation, nonadherent cells were removed carefully. Adherent cells were gently washed with prewarmed RPMI 1640 medium 4 times. Fluorescence was measured by using a fluorescence plate reader at 485 nm excitation. The number of THP-1 cells per view was also quantified from randomly acquired images.

Real-time qPCR. HUVECs were suspended in TRIzol reagent (Invitrogen), and total RNA was isolated according to the manufacturer's instructions. Reverse transcriptions were performed by using miScript Reverse Transcription Kit (218061; QIAGEN). Either QuantiTect SYBR Green RT-PCR Kit (204243; QIAGEN) or miScript SYBR Green PCR Kit (218073; QIAGEN) was used for real-time qPCR analysis with the Mx3000P Real-Time PCR System (Stratagene) following the manufacturer's instructions. Gene- and species-specific primers were used to detect human or mouse VCAM-1, E-selectin, PAI-1, and ICAM-1. To amplify mature miRNA sequences, hsa–miR-181a (PN4373117), hsa–miR-181b (PN4373116), hsa–miR-181c (PN4373115), hsa–miR-181d (PN4373180), RNU6B (PN4373381), TaqMan MicroRNA Reverse Transcription Kit (PN4366596), TaqMan Universal PCR Master Mix, No AmpErase UNG (PN4324018), or miScript primer assays for Hs_RN5S1_1 (MS00007574) and Hs_miR-181b_1 (MS00006699) from QIAGEN were used. Please see Supplemental Tables 1 and 2.

miRNA microarray, DNA microarray gene chip analysis, and bioinformatics. HUVECs were treated with 10 ng/ml TNF-α for 4 hours and collected into TRIzol; total RNAs were prepared for miRNA microarray analysis (LC Sciences). For DNA microarray gene chip analysis, HUVECs were transfected with 10 nM miRNA negative control or miR-181b mimics for 36 hours and treated with 10 ng/ml TNF-α for 4 hours. Cells were collected into TRIzol and sent for Two-Color, 4 × 44 K format, Human Whole Genome Microarray Service (Miltenyi Biotec Inc.). Microarray data have been deposited in the GEO database (accession no. GSE35030). Differentially expressed genes were identified by using the fold change lower threshold of 1.5. GSEA (57) was used to determine whether a known biological pathway/process or molecular function was suppressed by overexpression of miR-181b. Gene sets used for enrichment analyses were downloaded directly from the Broad Institute web site (www.broadinstitute.org/gsea/msigdb/index.jsp) or the Gene Ontology web site (http://www.geneontology.org/). Gene sets discovered with a false discovery rate (FDR) of less than 25% were considered as significantly enriched. The primers used for real-time qPCR validation are listed in Supplemental Table 2.

In vivo miR-181b overexpression or inhibition and animal experiments. Animals were housed in pathogen-free barrier facilities and regularly monitored by the veterinary staff. Male C57BL/6 mice from 8 to 10 weeks old were purchased from Charles River. An equal volume of atelocollagen and miRNAs (Ambion) was mixed to form complexes, according to the manufacturer's guidelines. Each mouse (n = 3–6 per group) was administered 200 μl mixtures containing 50 μg negative control or miR-181b mimics (~1 nmol/mouse) by tail-vein injection. Recombinant mouse TNF-α (2 μg/mouse) from R&D Systems (410-MT/CF) was i.p. injected on the following day. Four hours later, mice were sacrificed to harvest tissues and organs for analysis. Lungs were used for Western blot analysis, total RNA extraction, and immunohistochemistry. Aorta arches were snap-frozen for total RNA extraction, while the descending aorta was fixed with 4% paraformaldehyde and embedded in paraffin for immunohistochemistry. Hearts, spleens, and livers were used for total RNA isolation. Sections of 6 μm were prepared from paraffin-embedded lung and aorta; sections were then deparaffinized with xylene and rehydrated in water through a graded ethanol series, followed by antigen retrieval performed for 5 minutes in a pressure cooker using Tris-EDTA solution, pH 8.0. The sections were treated with TBST buffer and 3% H_2O_2, blocked with blocking reagent, incubated sequentially with goat anti-mouse VCAM-1, or anti–importin-α3 (ab6039; Abcam), secondary antibody, and substrates, and counterstained with hematoxylin. Images of staining in paraffin sections from vehicle (n = 3), miRNA negative control (n = 5), or miR-181b mimics–treated mice (n = 5) were acquired with an Olympus FluoView FV1000 microscope at ×40 magnification. The percentage of VCAM-1 or importin-α3 positivity along the endothelium (1 slide per mouse; 3 random fields) was measured using computer-assisted image analysis (Image-Pro Plus software; Media Cybernetics) by 2 blinded observers. Lung injury was evaluated from H&E staining by a blinded pathologist using a lung injury score as follows: score 0, no lung injury; score 0.1 to 2.5, mild-to-moderate lung injury; score 2.6 to 4.0, severe lung injury.

For the murine endotoxemia model, mice were administered vehicle (atelocollagen), miRNA negative control, or miR-181b mimics (50 μg/mouse) by tail-vein injection. On the following day, mice were i.p. injected with 40 mg/kg LPS (*E. coli* serotype 026:B6 endotoxin; Sigma-Aldrich) or vehicle

(saline). Lung tissues were processed for immunohistochemistry 4 hours after LPS treatment and stained for Gr-1 (BD Biosciences — Pharmingen), CD45 (BD Biosciences — Pharmingen), or VCAM-1. Myeloperoxidase (MPO) activity was measured in lung homogenates using the Amplex Red Peroxidase Assay Kit (Invitrogen) according to the manufacturer's instructions. In a separate experiment, 6-week-old male C57BL/6 mice were injected i.v. with vehicle, miRNA negative control, or miR-181b mimics (1 nmol/mouse) at 48 and 24 hours before and 1.5 hours after LPS administration (50 mg per kg i.p., n = 10 to 11 per group), and monitored 6 times daily for survival. To determine the effect of miR-181b on NF-κB activation in vivo, 8- to 10-week-old C57BL/6 male mice were injected (i.v.) 3 times with a mixture of Lipofectamine 2000 and miR-181b mimics or miRNA NS negative controls on days 1, 2, and 3, and challenged with 10 mg/kg LPS (026:B6) on day 4 for 2 hours. Lungs were harvested for histological analysis and stained with DAPI, anti-CD31, and anti-p65 followed by secondary antibodies. Images were acquired on an upright Carl Zeiss LSM 510 confocal microscope equipped with Plan-Neofluar ×40/1.3 oil-immersion objective using the 405 nm diode laser, the 543 nm line of a HeNe543 laser, and the 633 nm line of a HeNe633 laser. Fluorescence intensity of nuclear p65 was measured using ImageJ software (http://rsbweb.nih.gov/ij/). NGL mice (NF-κB promoter with GFP/luciferase fusion reporter) fully backcrossed into C57BL/6 were reported previously (63, 64). Male 6- to 8-week-old mice were injected (i.v.) with a mixture of Lipofectamine 2000 and mimics (miRNA negative control, or miR-181b; 1 nmol/mouse) or inhibitors (miRNA inhibitor negative control, or miR-181b inhibitor; 2 nmol/mouse) 3 times on days 1, 2, and 3 and challenged with 10 mg/kg LPS (026:B6) on day 4 for 4 hours; tissues were harvested for analyses. NGL mice were injected with recombinant adenovirus, Ad-GFP, or Ad-DN-IκBα (expressing dominant-negative IκBα) at 3×10^9 PFU/mouse, followed by 3 mimics injections as described above. To measure luciferase activity, 400 μl 1× Reporter Lysis Buffer from Promega was added for a small piece of tissue (about 20 mg wet weight). The lysates were spun at 11,700 *g* for 5 minutes after homogenization, and 40 μl of lysate was loaded to measure luciferase activity.

Clinical sepsis plasma samples and real-time qPCR analysis. Human plasma samples were obtained from a prospectively enrolled cohort of patients admitted to the adult medical ICU Registry of Critical Illness in accordance with the Institutional Review Board–approved protocol at Brigham and Women's Hospital. Enrolled subjects were characterized as sepsis, sepsis plus ARDS, or control subjects (ICU patients without sepsis or ARDS) by a group of blinded critical care physicians. A subset of randomly selected subjects from the MICU Registry with the above diagnoses was selected for analysis. Anonymized plasma samples were generated from blood collected in EDTA-containing tubes obtained from patients within 24 to 48 hours of admission and stored at −80°C. Plasma was isolated from whole blood at 1500 *g* for 15 minutes at room temperature. No significant differences were observed for miR-181b expression in microparticle-enriched or nonenriched plasma in 3 healthy human subjects (data not shown). Total RNA was isolated from plasma by using the Total RNA Purification Kit from Norgen Biotek Corporation and reverse transcription and real-time qPCR were performed as described above. Human plasma samples were provided by the following MICU Registry members: Tamas Dolinay (University of Tennessee, Chattanooga, Tennessee, USA); and Lee Gazourian, Laura Fredenburgh, Anthony Massaro, Augustine Choi (Brigham and Women's Hospital).

Statistics. Differences between 2 groups were examined using Student's *t* test (2-tailed). Mann-Whitney *U* test was used to determine whether a difference exists between 2 groups for Figure 6B and Figure 8G. One-tailed log-rank test was used for Figure 6I. $P < 0.05$ was considered significant.

Study approval. Human study protocols were approved by the Institutional Review Board at Brigham and Women's Hospital. Written informed consent was obtained from all participants or their appropriate surrogates. All protocols concerning animal use were approved by the Institutional Animal Care and Use Committee at Harvard Medical School and conducted in accordance with the NIH Guide for the Care and Use of Laboratory Animals.

Acknowledgments

We acknowledge Yevgenia Tesmenitsky (Brigham and Women's Hospital) for technical help with some of the intravenous injections and Bonna Ith (Brigham and Women's Hospital) for technical help with Gr-1 staining. This work was supported by funding from the NIH (HL091076 and HL115141 to M.W. Feinberg; F32HL088819 to A.K.M. Wara), the American Cancer Society (Research Scholar Grant RSG0719501-LIB to M.W. Feinberg), the Boston Area Diabetes Endocrinology Research Center Pilot Grant P30DK057521 to M.W. Feinberg), and a Watkins Cardiovascular Medicine Discovery Award (to M.W. Feinberg).

Received for publication October 14, 2011, and accepted in revised form March 14, 2012.

Address correspondence to: Mark W. Feinberg, Department of Medicine, Cardiovascular Division, Brigham and Women's Hospital, Harvard Medical School, 77 Avenue Louis Pasteur, NRB-742F, Boston, Massachusetts 02115, USA. Phone: 617.525.4381; Fax: 617.525.4380; E-mail: mfeinberg@rics.bwh.harvard.edu.

1. Aird WC. The role of the endothelium in severe sepsis and multiple organ dysfunction syndrome. *Blood*. 2003;101(10):3765–3777.
2. Aird WC. Endothelium as a therapeutic target in sepsis. *Curr Drug Targets*. 2007;8(4):501–507.
3. Baker RG, Hayden MS, Ghosh S. NF-kappaB, inflammation, and metabolic disease. *Cell Metab*. 2011;13(1):11–22.
4. Gareus R, et al. Endothelial cell-specific NF-kappaB inhibition protects mice from atherosclerosis. *Cell Metab*. 2008;8(5):372–383.
5. Guerci B, Bohme P, Kearney-Schwartz A, Zannad F, Drouin P. Endothelial dysfunction and type 2 diabetes. Part 2: altered endothelial function and the effects of treatments in type 2 diabetes mellitus. *Diabetes Metab*. 2001;27(4 pt 1):436–447.
6. Hansson GK, Libby P. The immune response in atherosclerosis: a double-edged sword. *Nat Rev Immunol*. 2006;6(7):508–519.
7. Khan F, Galarraga B, Belch JJ. The role of endothelial function and its assessment in rheumatoid arthritis. *Nat Rev Rheumatol*. 2010;6(5):253–261.
8. Roifman I, et al. Evidence of endothelial dysfunction in patients with inflammatory bowel disease. *Clin Gastroenterol Hepatol*. 2009;7(2):175–182.
9. Ley K, Laudanna C, Cybulsky MI, Nourshargh S. Getting to the site of inflammation: the leukocyte adhesion cascade updated. *Nat Rev Immunol*. 2007;7(9):678–689.
10. Pober JS, Sessa WC. Evolving functions of endothelial cells in inflammation. *Nat Rev Immunol*. 2007;7(10):803–815.
11. Shapiro NI, et al. The association of endothelial cell signaling, severity of illness, and organ dysfunction in sepsis. *Crit Care*. 2010;14(5):R182.
12. Xu DY, Zhao SP, Peng WP. Elevated plasma levels of soluble P-selectin in patients with acute myocardial infarction and unstable angina. An inverse link to lipoprotein(a). *Int J Cardiol*. 1998;64(3):253–258.
13. Hou J, Baichwal V, Cao Z. Regulatory elements and transcription factors controlling basal and cytokine-induced expression of the gene encoding intercellular adhesion molecule 1. *Proc Natl Acad Sci U S A*. 1994;91(24):11641–11645.
14. Montgomery KF, et al. Activation of endothelial-leukocyte adhesion molecule 1 (ELAM-1) gene transcription. *Proc Natl Acad Sci U S A*. 1991;88(15):6523–6527.
15. Neish AS, Williams AJ, Palmer HJ, Whitley MZ, Collins T. Functional analysis of the human vascular cell adhesion molecule 1 promoter. *J Exp Med*. 1992;176(6):1583–1593.
16. Pober JS, Bevilacqua MP, Mendrick DL, Lapierre LA, Fiers W, Gimbrone MA Jr. Two distinct monokines, interleukin 1 and tumor necrosis factor, each independently induce biosynthesis and transient expression of the same antigen on the surface of cultured human vascular endothelial cells. *J Immunol*. 1986;136(5):1680–1687.
17. Manning AM, et al. NF-kappa B is activated during acute inflammation in vivo in association with elevated endothelial cell adhesion molecule gene expression and leukocyte recruitment. *J Inflamm*. 1995;45(4):283–296.

18. Ghosh S, Hayden MS. New regulators of NF-kappaB in inflammation. *Nat Rev Immunol*. 2008; 8(11):837–848.
19. Perkins ND. Integrating cell-signalling pathways with NF-kappaB and IKK function. *Nat Rev Mol Cell Biol*. 2007;8(1):49–62.
20. Karin M, Ben-Neriah Y. Phosphorylation meets ubiquitination: the control of NF-[kappa]B activity. *Annu Rev Immunol*. 2000;18:621–663.
21. Kempe S, Kestler H, Lasar A, Wirth T. NF-kappaB controls the global pro-inflammatory response in endothelial cells: evidence for the regulation of a pro-atherogenic program. *Nucleic Acids Res*. 2005;33(16):5308–5319.
22. Molestina RE, Miller RD, Lentsch AB, Ramirez JA, Summersgill JT. Requirement for NF-kappaB in transcriptional activation of monocyte chemotactic protein 1 by Chlamydia pneumoniae in human endothelial cells. *Infect Immun*. 2000;68(7):4282–4288.
23. Zhou Z, Connell MC, MacEwan DJ. TNFR1-induced NF-kappaB, but not ERK, p38MAPK or JNK activation, mediates TNF-induced ICAM-1 and VCAM-1 expression on endothelial cells. *Cell Signal*. 2007;19(6):1238–1248.
24. Hajra L, Evans AI, Chen M, Hyduk SJ, Collins T, Cybulsky MI. The NF-kappa B signal transduction pathway in aortic endothelial cells is primed for activation in regions predisposed to atherosclerotic lesion formation. *Proc Natl Acad Sci U S A*. 2000;97(16):9052–9057.
25. Blackwell TS, Christman JW. The role of nuclear factor-kappa B in cytokine gene regulation. *Am J Respir Cell Mol Biol*. 1997;17(1):3–9.
26. Cuhlmann S, et al. Disturbed blood flow induces RelA expression via c-Jun N-terminal kinase 1: a novel mode of NF-kappaB regulation that promotes arterial inflammation. *Circ Res*. 2011;108(8):950–959.
27. O'Connell RM, Rao DS, Chaudhuri AA, Baltimore D. Physiological and pathological roles for microRNAs in the immune system. *Nat Rev Immunol*. 2010;10(2):111–122.
28. Taganov KD, Boldin MP, Chang KJ, Baltimore D. NF-kappaB-dependent induction of microRNA miR-146, an inhibitor targeted to signaling proteins of innate immune responses. *Proc Natl Acad Sci U S A*. 2006;103(33):12481–12486.
29. Bartel DP. MicroRNAs: target recognition and regulatory functions. *Cell*. 2009;136(2):215–233.
30. Guo H, Ingolia NT, Weissman JS, Bartel DP. Mammalian microRNAs predominantly act to decrease target mRNA levels. *Nature*. 2010;466(7308):835–840.
31. Valencia-Sanchez MA, Liu J, Hannon GJ, Parker R. Control of translation and mRNA degradation by miRNAs and siRNAs. *Genes Dev*. 2006; 20(5):515–524.
32. Baek D, Villen J, Shin C, Camargo FD, Gygi SP, Bartel DP. The impact of microRNAs on protein output. *Nature*. 2008;455(7209):64–71.
33. Griffiths-Jones S. The microRNA Registry. *Nucleic Acids Res*. 2004;32(Database issue):D109–D111.
34. Fang Y, Shi C, Manduchi E, Civelek M, Davies PF. MicroRNA-10a regulation of proinflammatory phenotype in athero-susceptible endothelium in vivo and in vitro. *Proc Natl Acad Sci U S A*. 2010;107(30):13450–13455.
35. Suarez Y, Wang C, Manes TD, Pober JS. Cutting edge: TNF-induced microRNAs regulate TNF-induced expression of E-selectin and intercellular adhesion molecule-1 on human endothelial cells: feedback control of inflammation. *J Immunol*. 2010; 184(1):21–25.
36. Bevilacqua MP, Pober JS, Mendrick DL, Cotran RS, Gimbrone MA Jr. Identification of an inducible endothelial-leukocyte adhesion molecule. *Proc Natl Acad Sci U S A*. 1987;84(24):9238–9242.
37. Pober JS, et al. Activation of cultured human endothelial cells by recombinant lymphotoxin: comparison with tumor necrosis factor and interleukin 1 species. *J Immunol*. 1987;138(10):3319–3324.
38. Dustin ML, Rothlein R, Bhan AK, Dinarello CA, Springer TA. Induction by IL 1 and interferon-gamma: tissue distribution, biochemistry, and function of a natural adherence molecule (ICAM-1). *J Immunol*. 1986;137(1):245–254.
39. Behm CZ, et al. Molecular imaging of endothelial vascular cell adhesion molecule-1 expression and inflammatory cell recruitment during vasculogenesis and ischemia-mediated arteriogenesis. *Circulation*. 2008;117(22):2902–2911.
40. Kaufmann BA, et al. Molecular imaging of the initial inflammatory response in atherosclerosis: implications for early detection of disease. *Arterioscler Thromb Vasc Biol*. 2010;30(1):54–59.
41. Kaufmann BA, et al. Molecular imaging of inflammation in atherosclerosis with targeted ultrasound detection of vascular cell adhesion molecule-1. *Circulation*. 2007;116(3):276–284.
42. Lindner JR. Molecular imaging of cardiovascular disease with contrast-enhanced ultrasonography. *Nat Rev Cardiol*. 2009;6(7):475–481.
43. Hoefen RJ, Berk BC. The role of MAP kinases in endothelial activation. *Vascul Pharmacol*. 2002; 38(5):271–273.
44. Oeckinghaus A, Ghosh S. The NF-kappaB family of transcription factors and its regulation. *Cold Spring Harb Perspect Biol*. 2009;1(4):a000034.
45. Vallabhapurapu S, Karin M. Regulation and function of NF-kappaB transcription factors in the immune system. *Annu Rev Immunol*. 2009;27:693–733.
46. Berk BC, Abe JI, Min W, Surapisitchat J, Yan C. Endothelial atheroprotective and anti-inflammatory mechanisms. *Ann N Y Acad Sci*. 2001;947:93–109.
47. Read MA, et al. Tumor necrosis factor alpha-induced E-selectin expression is activated by the nuclear factor-kappaB and c-JUN N-terminal kinase/p38 mitogen-activated protein kinase pathways. *J Biol Chem*. 1997;272(5):2753–2761.
48. Surapisitchat J, Hoefen RJ, Pi X, Yoshizumi M, Yan C, Berk BC. Fluid shear stress inhibits TNF-alpha activation of JNK but not ERK1/2 or p38 in human umbilical vein endothelial cells: Inhibitory crosstalk among MAPK family members. *Proc Natl Acad Sci U S A*. 2001;98(11):6476–6481.
49. Fagerlund R, Kinnunen L, Kohler M, Julkunen I, Melen K. NF-{kappa}B is transported into the nucleus by importin {alpha}3 and importin {alpha}4. *J Biol Chem*. 2005;280(16):15942–15951.
50. Fagerlund R, Melen K, Cao X, Julkunen I. NF-kappaB p52, RelB and c-Rel are transported into the nucleus via a subset of importin alpha molecules. *Cell Signal*. 2008;20(8):1442–1451.
51. Kohler M, et al. Evidence for distinct substrate specificities of importin alpha family members in nuclear protein import. *Mol Cell Biol*. 1999;19(11):7782–7791.
52. Lewis BP, Burge CB, Bartel DP. Conserved seed pairing, often flanked by adenosines, indicates that thousands of human genes are microRNA targets. *Cell*. 2005;120(1):15–20.
53. Kertesz M, Iovino N, Unnerstall U, Gaul U, Segal E. The role of site accessibility in microRNA target recognition. *Nat Genet*. 2007;39(10):1278–1284.
54. John B, Enright AJ, Aravin A, Tuschl T, Sander C, Marks DS. Human microRNA targets. *PLoS Biol*. 2004;2(11):e363.
55. Miranda KC, et al. A pattern-based method for the identification of microRNA binding sites and their corresponding heteroduplexes. *Cell*. 2006; 126(6):1203–1217.
56. Lal A, et al. miR-24 Inhibits cell proliferation by targeting E2F2, MYC, and other cell-cycle genes via binding to "seedless" 3′UTR microRNA recognition elements. *Mol Cell*. 2009;35(5):610–625.
57. Subramanian A, et al. Gene set enrichment analysis: a knowledge-based approach for interpreting genome-wide expression profiles. *Proc Natl Acad Sci U S A*. 2005;102(43):15545–15550.
58. Lever A, Mackenzie I. Sepsis: definition, epidemiology, and diagnosis. *BMJ*. 2007;335(7625):879–883.
59. Annane D, Bellissant E, Cavaillon JM. Septic shock. *Lancet*. 2005;365(9453):63–78.
60. Lu YC, Yeh WC, Ohashi PS. LPS/TLR4 signal transduction pathway. *Cytokine*. 2008;42(2):145–151.
61. Nduka OO, Parrillo JE. The pathophysiology of septic shock. *Crit Care Clin*. 2009;25(4):677–702, vii.
62. Woodman RC, Teoh D, Payne D, Kubes P. Thrombin and leukocyte recruitment in endotoxemia. *Am J Physiol Heart Circ Physiol*. 2000;279(3):H1338–H1345.
63. Everhart MB, et al. Duration and intensity of NF-kappaB activity determine the severity of endotoxin-induced acute lung injury. *J Immunol*. 2006; 176(8):4995–5005.
64. Lawson WE, et al. Endoplasmic reticulum stress enhances fibrotic remodeling in the lungs. *Proc Natl Acad Sci U S A*. 2011;108(26):10562–10567.
65. Ji X, Takahashi R, Hiura Y, Hirokawa G, Fukushima Y, Iwai N. Plasma miR-208 as a biomarker of myocardial injury. *Clin Chem*. 2009;55(11):1944–1949.
66. Mitchell PS, et al. Circulating microRNAs as stable blood-based markers for cancer detection. *Proc Natl Acad Sci U S A*. 2008;105(30):10513–10518.
67. Recchiuti A, Krishnamoorthy S, Fredman G, Chiang N, Serhan CN. MicroRNAs in resolution of acute inflammation: identification of novel resolvin D1-miRNA circuits. *FASEB J*. 2011;25(2):544–560.
68. Knaus WA, Draper EA, Wagner DP, Zimmerman JE. APACHE II: a severity of disease classification system. *Crit Care Med*. 1985;13(10):818–829.
69. Berlin C, et al. alpha 4 integrins mediate lymphocyte attachment and rolling under physiologic flow. *Cell*. 1995;80(3):413–422.
70. Bevilacqua MP, Stengelin S, Gimbrone MA Jr, Seed B. Endothelial leukocyte adhesion molecule 1: an inducible receptor for neutrophils related to complement regulatory proteins and lectins. *Science*. 1989;243(4895):1160–1165.
71. Kansas GS. Selectins and their ligands: current concepts and controversies. *Blood*. 1996; 88(9):3259–3287.
72. Chen CZ, Li L, Lodish HF, Bartel DP. MicroRNAs modulate hematopoietic lineage differentiation. *Science*. 2004;303(5654):83–86.
73. Li QJ, et al. miR-181a is an intrinsic modulator of T cell sensitivity and selection. *Cell*. 2007; 129(1):147–161.
74. Kazenwadel J, Michael MZ, Harvey NL. Prox1 expression is negatively regulated by miR-181 in endothelial cells. *Blood*. 2010;116(13):2395–2401.
75. de Yebenes VG, et al. miR-181b negatively regulates activation-induced cytidine deaminase in B cells. *J Exp Med*. 2008;205(10):2199–2206.
76. Ma X, Becker Buscaglia LE, Barker JR, Li Y. MicroRNAs in NF-kappaB signaling. *J Mol Cell Biol*. 2011;3(3):159–166.
77. Marcucci G, et al. MicroRNA expression in cytogenetically normal acute myeloid leukemia. *N Engl J Med*. 2008;358(18):1919–1928.
78. Schaefer A, et al. Diagnostic and prognostic implications of microRNA profiling in prostate carcinoma. *Int J Cancer*. 2010;126(5):1166–1176.
79. Schwind S, et al. Prognostic significance of expression of a single microRNA, miR-181a, in cytogenetically normal acute myeloid leukemia: a Cancer and Leukemia Group B study. *J Clin Oncol*. 2010; 28(36):5257–5264.
80. Slaby O, et al. MicroRNA-181 family predicts response to concomitant chemoradiotherapy with temozolomide in glioblastoma patients. *Neoplasma*. 2010;57(3):264–269.
81. Visone R, et al. miR-181b is a biomarker of disease progression in chronic lymphocytic leukemia. *Blood*. 2011;118(11):3072–3079.
82. Zhi F, et al. The use of hsa-miR-21, hsa-miR-181b and hsa-miR-106a as prognostic indicators of astrocytoma. *Eur J Cancer*. 2010;46(9):1640–1649.

83. Chen G, et al. MicroRNA-181a sensitizes human malignant glioma U87MG cells to radiation by targeting Bcl-2. *Oncol Rep*. 2010;23(4):997–1003.
84. Zhu W, Shan X, Wang T, Shu Y, Liu P. miR-181b modulates multidrug resistance by targeting BCL2 in human cancer cell lines. *Int J Cancer*. 2010; 127(11):2520–2529.
85. Shi L, et al. hsa-mir-181a and hsa-mir-181b function as tumor suppressors in human glioma cells. *Brain Res*. 2008;1236:185–193.
86. Marcucci G, et al. Prognostic significance of, and gene and microRNA expression signatures associated with, CEBPA mutations in cytogenetically normal acute myeloid leukemia with high-risk molecular features: a Cancer and Leukemia Group B Study. *J Clin Oncol*. 2008;26(31):5078–5087.
87. Schetter AJ, et al. MicroRNA expression profiles associated with prognosis and therapeutic outcome in colon adenocarcinoma. *JAMA*. 2008;299(4):425–436.
88. Iliopoulos D, Jaeger SA, Hirsch HA, Bulyk ML, Struhl K. STAT3 activation of miR-21 and miR-181b-1 via PTEN and CYLD are part of the epigenetic switch linking inflammation to cancer. *Mol Cell*. 2010;39(4):493–506.
89. Wang B, et al. TGFbeta-mediated upregulation of hepatic miR-181b promotes hepatocarcinogenesis by targeting TIMP3. *Oncogene*. 2010;29(12):1787–1797.
90. Liu G, Min H, Yue S, Chen CZ. Pre-miRNA loop nucleotides control the distinct activities of mir-181a-1 and mir-181c in early T cell development. *PLoS One*. 2008;3(10):e3592.
91. Harris TA, Yamakuchi M, Ferlito M, Mendell JT, Lowenstein CJ. MicroRNA-126 regulates endothelial expression of vascular cell adhesion molecule 1. *Proc Natl Acad Sci U S A*. 2008;105(5):1516–1521.
92. Theiss AL, Jenkins AK, Okoro NI, Klapproth JM, Merlin D, Sitaraman SV. Prohibitin inhibits tumor necrosis factor alpha-induced nuclear factor-kappa B nuclear translocation via the novel mechanism of decreasing importin alpha3 expression. *Mol Biol Cell*. 2009;20(20):4412–4423.
93. Kobayashi-Sakamoto M, Hirose K, Isogai E, Chiba I. NF-kappaB-dependent induction of osteoprotegerin by Porphyromonas gingivalis in endothelial cells. *Biochem Biophys Res Commun*. 2004;315(1):107–112.
94. Schwenzer R, et al. The human tumor necrosis factor (TNF) receptor-associated factor 1 gene (TRAF1) is up-regulated by cytokines of the TNF ligand family and modulates TNF-induced activation of NF-kappaB and c-Jun N-terminal kinase. *J Biol Chem*. 1999;274(27):19368–19374.
95. Wei S, Kitaura H, Zhou P, Ross FP, Teitelbaum SL. IL-1 mediates TNF-induced osteoclastogenesis. *J Clin Invest*. 2005;115(2):282–290.
96. Vasilescu C, et al. MicroRNA fingerprints identify miR-150 as a plasma prognostic marker in patients with sepsis. *PLoS One*. 2009;4(10):e7405.
97. Wang JF, et al. Serum miR-146a and miR-223 as potential new biomarkers for sepsis. *Biochem Biophys Res Commun*. 2010;394(1):184–188.